

von Karman Institute for Fluid Dynamics
Chaussée de Waterloo, 72
B - 1640 Rhode Saint Genèse - Belgium

Project Report

Numerical study of the effect of the gas to wall temperature ratio on
the bypass transition

Riccardo Rubini

Supervisor:
Tony Arts
Advisor:
Roberto Maffulli

June 2017

Acknowledgments

Here we are at the end also of this adventure, after this intense year there are a lot of people that contributed in a way of an other to my project. First of all I want to thanks my advisor Roberto Maffulli for the patience and the wisdom with which he has been able to suggest me from the very beginning to the very end of the project. I am very grateful to have had the opportunity to learn a lot of very important things (not only related to the fluid dynamics, that's the extra value). A great thanks goes also to Professor Tony Arts, there are no words to describe his kindness and patience from the personal point of view and his wisdom and deep knowledge from the technical one. At last but not the least I would like to thanks all my fellow research master companions that contribute to makes this amazing experience at von Karman Institutue much more awesome.

Abstract

The study of boundary layer transition plays a fundamental role in the field of turbomachinery; the main reason is the strong influence of the transition on the flow field local parameters such as skin friction and heat transfer, this variation of the local parameters is reflected on global ones such as overall efficiency of the blade row and of the machine. The understanding of the laminar turbulent phenomenon can help designers to improve aerodynamic and thermodynamic performances of components and of the whole machine. Transition models are nowadays commonly used tools in both CFD research and design practice. It is then of particular interest to understand if the commonly used transition models can predict the effect of temperature on bypass transition and, in case of positive answer, the reasons of their behaviour. This becomes particularly interesting as commonly used transition models start from assumptions that are unlikely to be verified in the considered environment. The chosen transition models are: the $\gamma - Re_\theta$ of Menter and Langtry and $k - k_l - \omega$ of Walters and Cokljat because of the different kind of approach to the same problem. In order to isolate the effects of the temperature ratio on the transition the simulations have been performed keeping the same values of Reynolds and Mach number and reaching the desired value of the temperature ratio varying the freestream or varying the blade temperature. Then the results have been compared between them in order to check the consistency of the models and then compared to experimental results in order to understand their capabilities in describing the real physics. The results obtained are quite encouraging for the $k - k_l - \omega$ that shows to be able to reproduce, although in a qualitative way, the behaviour observed in the experimental campaign.

Contents

List of Figures	vii
List of Tables	ix
List of Symbols	xi
1 Introduction	1
1.1 Transition modes	1
1.2 Transition in Turbomachinery	2
1.3 Outline of the project	3
2 Bibliographic Review	5
2.1 Thermal effects on boundary layer	5
2.2 Natural transition studies	6
2.3 Bypass transition studies	8
2.4 Conclusions	10
3 Transition Models	13
3.1 General idea behind the RANS transition models	13
3.2 $\gamma - Re_\theta$	14
3.2.1 Vorticity Reynolds number as onset transition criterion	14
3.2.2 Transport equation for Intermittency	15
3.2.3 Transport equation for the transition momentum thickness Reynolds number	16
3.2.4 Coupling with existing turbulence model	17
3.3 $k - k_l - \omega$	17
3.3.1 Phenomenology of transition	17
3.3.2 Model formulation	18
3.4 Final remarks	20
4 Numerical set up and Validation	21
4.1 Space discretization	21
4.2 Time discretization	22
4.3 Mesh and computational domain	23

4.3.1 $\gamma - Re_\theta$ grid independence	23
4.4 Aerodynamic and thermal validation	25
4.4.1 $k - k_l - \omega$ grid independence	27
4.5 Remarks	27
5 Results	29
5.1 Preliminary aerodynamic study	29
5.2 Experimental results at low turbulence intensity	30
5.3 $\gamma - Re_\theta$ with $T_{wall} = 294[K]$	31
5.3.1 Velocity profile	33
5.3.2 Density and viscosity	34
5.3.3 Turbulent quantities	36
5.4 $\gamma - Re_\theta$ with $T_0 = 441[K]$	37
5.4.1 Kinematic quantities	38
5.4.2 Density and viscosity	38
5.4.3 Turbulent quantities	41
5.4.4 $\gamma - Re_\theta$ Conclusions	41
5.5 $k - k_l - \omega$	43
5.5.1 $k - k_l - \omega$ $T_{wall} = 294$	44
5.5.2 Velocity	45
5.5.3 Density and viscosity	45
5.5.4 Turbulent variables	47
5.5.5 $k - k_l - \omega$ $T_0 = 441$	49
5.5.6 Velocity	50
5.5.7 Density and viscosity	51
5.5.8 Turbulent variables	51
5.5.9 $k - k_l - \omega$ Conclusions	53
5.6 Experimental results with high free stream turbulence intensity	54
6 Conclusions and future work	57
6.1 Conclusions	57
6.1.1 $\gamma - Re_\theta$	57
6.1.2 $k - k_l - \omega$	58
6.2 Future works	58
A Annex A	61
A.1 Boundary Condition Conversion	61
A.2 Turbulent boundary conditions	63
B Appendix B	67
References	69

List of Figures

1.1	Natural and Bypass Transition Process	2
1.2	Heat Transfer Coefficient along the Pressure and Suction side of a nozzle guide vain	3
2.1	Influence of free stream pressure gradient on the turbulent Prandtl number [26]	6
2.2	Stability region for incompressible and not isothermal boundary layer [21]	7
2.3	a) Velocity Profile b) curvature of Velocity profile [21]	7
2.4	Location of the thin film and time resolved heat flux [10]	9
2.5	Heat transfer distribution for different temperature ratio [16]	10
4.1	Computational Domain around the profile	23
4.2	Mesh	24
4.3	Details at TE a) and of the periodic connections b)	24
4.4	Distribution along the blade PS and SS	25
4.5	Distribution of the heat transfer coefficient for two different value of free stream turbulence intensity Tu=1% and 6%	26
4.6	Isoentropic Mach number distribution	27
4.7	$k - k_l - \omega$	28
5.1	Isoentropic Mach Number distribution at different value of M_{2iso}	30
5.2	Heat Transfer Coefficient From the Experiments	31
5.3	Heat Transfer Coefficient From the Experiments	32
5.4	Location of the cuts	33
5.5	Absolute Velocity	33
5.6	Dynamic Viscosity	34
5.7	Density	35
5.8	Kinematic Viscosity	35
5.9	Intermittency	36
5.10	Momentum Thickness Reynolds Number	37
5.11	Heat transfer coefficient at constant Free Stream conditions	38
5.12	Velocity distribution inside the boundary layer at constant free stream conditions	39

5.13	Dynamic Viscosity	39
5.14	Density	40
5.15	Kinematic Viscosity	40
5.16	Intermittency	41
5.17	Momentum Thickness Reynolds Number	42
5.18	Vorticity Reynolds number for the case at constant wall temperature . . .	43
5.19	Vorticity Reynolds Number for the case at constant FS temperature . . .	44
5.20	Heat Transfer coefficient	45
5.21	Absolute Velocity	46
5.22	Density	46
5.23	Dynamic Viscosity	47
5.24	Kinematic viscosity	47
5.25	Laminar Kinetic Energy	48
5.26	Turbulent Kinetic Energy	48
5.27	Energy Transfer	49
5.28	Heat Transfer coefficient	50
5.29	Absolute Velocity	50
5.30	Kinematic viscosity	51
5.31	Turbulent Kinetic Energy	52
5.32	Laminar Kinetic Energy	52
5.33	Energy Transfer	53
5.34	Heat Transfer Coefficient from the experiment left and computation right	55
A.1	Decay of a) turbulent kinetic energy b) specific dissipation from the inlet section from the LE	66
B.1	Planning of the Project	68

List of Tables

4.1	Boundary conditions for the thermal validation of the $\gamma - Re_\theta$ measured by [5]	25
4.2	Boundary conditions for the aerodynamic validation of the $\gamma - Re_\theta$ for comparison with [5]	26
4.3	Boundary conditions for the thermal validation of $k - k_{l-\omega}$ computation, measurement from [5]	27
5.1	Boundary condition measured in the facility for the case at low turbulence intensity and low $FSTI$	31
5.2	Boundary conditions for the $\gamma - Re_\theta$ at wall temperature constant and low $FSTI$	31
5.3	Locations in the percentage on the suction side of the cuts' location	32
5.4	Boundary conditions for the $\gamma - Re_\theta$ at free stream conditions constant and low $FSTI$	37
5.5	Boundary conditions for the $k - k_l - \omega$ at wall temperature constant and low $FSTI$	44
5.6	Boundary conditions for the $k - k_{l-\omega}$ at free stream conditions constant and low $FSTI$	49
5.7	Boundary conditions for the case at high turbulence intensity	54

List of Symbols

Acronyms

RANS	Reynolds Average Navier Stokes
CFD	Computational fluid dynamics
HTC	Heat transfer coefficient
SST	Shear Stress Transport
N-S	Navier Stokes equations
BP	Bypass Transition
NAT	Natural Transition
VKI	von Karman Institute
RM	Research Master
BC	Boundary conditions
LES	Large Eddy Simulation
LE	Leading Edge
TE	Trailing Edge
PS	Pressure Side
SS	Suction Side

Roman symbols

k, k_T	Turbulent kinetic energy	$\frac{m^2}{s^2}$
k_l	laminar kinetic energy	$\frac{m^2}{s^2}$
Pr_T	Turbulent Prandtl number	-
Re	Reynolds number	-
$y+$	Non dimensional wall distance	-
p	Pressure	Pa
L_t	Turbulence integral length scale	m
q	Specific heat flux	W/m^2
y, d	Dimensional wall distance	m
T	temperature	K
u	x -(tangential) components of velocity	m/s
U	Absolute value of the velocity	m/s
v	specific volume	m^3/kg
v	y- (radial) component of velocity	m/s
w	z- (axial) component of velocity	m/s
Re_θ	momentum thickness Reynolds number	-
Re_v	vorticity Reynolds number	-
S	Norm of the strain tensor	$\frac{1}{s}$
Tu	Turbulence Intensity	-
H	Heat transfer coefficient	$\frac{W}{m^2k}$
S	Curvilinear abscissa	m
$\tilde{Re}_{\theta t}$	momentum thickness transition Reynolds number	-
M_{iso}	Isoentropic Mach number	-
P_i	Production term	-
D_i	Destruction term	-
R_{BP}	Energy transport term for bypass transition	$\frac{m^2}{s^3}$
R_{NP}	Energy transport term for natural transition	$\frac{m^2}{s^3}$
N	Number of point	-
V	Volume	m^3

Greek symbols

θ	Momentum thickness	m
γ	Intermittency function	-
ω	Turbulence frequency	$\frac{1}{s}$
δ	Boundary layer thickness	m
α	Wave number	$\frac{1}{m}$
ρ	Density	kg/m^3
Ω	Module of vorticity	$\frac{1}{m}$
μ	Dynamic viscosity	Pas
ν	Kinematic viscosity	$\frac{m^2}{s}$
λ	Non-dimensional free stream pressure gradient	-
ϕ	Threshold function	-
Σ	Surface	m^2
γ	Specific heat ratio	-

Sub- and Superscripts

<i>iso</i>	Isoentropic
<i>v</i>	Viscous
<i>d</i>	Dynamic
<i>lam</i>	Laminar
<i>turb</i>	Turbulent
0	Total inlet value
2	Outlet value
<i>w</i>	Value referred to the wall
<i>ratio</i>	Ratio total wall quantities $\frac{T_0}{T_w}$
∞	Freestream value
<i>exp</i>	Experimental results
<i>H</i>	referred to the thermal boundary layer

Chapter 1

Introduction

Boundary layer transition is a very complex phenomenon that takes place very often in the engineering flows affecting in a serious way the performances of the device both from an aerodynamic and from a thermal point of view. The development of transition is the result of the inception and the exponential growth of flow instabilities that can finally breakdown to turbulence. The study of transitional flow is very interesting from a physical perspective in order to try to archive a fully detailed description of the flow features. Moreover a deeper understanding of the physical phenomenon can also help the engineering to develop reduced order models able to describe in a more precise way the effects that the local parameters have on the global features of the flow fields such as drag coefficient a heat transfer.

1.1 Transition modes

One of the most difficult and still not understood characteristics of the transitional flows is the physical mechanism behind the inception and the development of the transitional flows. This lack of knowledge lead to a classification of three principal ways according to which the transitional flows can develop.

Natural Transition

It is quite generally accepted that in the presence of very low environmental disturbances and when a certain value of Reynolds number is reached the flow became unstable a certain number of longitudinal disturbances start to grow in amplitude. Usually transition occurs when the waves become nonlinear producing three dimensional structures [25]. At this point the three dimensional structures break down generating turbulent spots inside the laminar flow. In the last phase the turbulent spots coalesce into a fully turbulent flow. One of the main tool used to describe this kind of transition is the linear stability theory, the main limit of this approach is able to describe only the inception of the instability process but not its evolution.

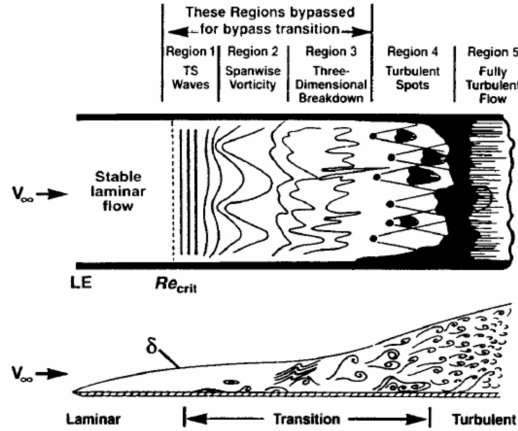


Figure 1.1: Natural and Bypass Transition Process

Bypass Transition

If the free stream perturbations are higher it is possible that the first second and third stage of the natural transition are bypassed an the turbulent spots are directly produced (Fig. 1.1 due to the influence of the free stream disturbances [17] [22]. It is also important to notice that the bypass transition can also occur because of the surface roughness where the perturbation is generated by the wall instead of from the free stream turbulence. Another location when the bypass transition is likely to occur is near the location of the cooling holes in a turbine stator or rotor blade because of the presence of the hole itself and the injection of turbulent flow inside the boundary layer. It is important to underline that the framework of the linear stability theory is completely meaningless in describing this kind of phenomenon, for this reason a completely different set of tools must be developed to describe these flow conditions very representative of the greater part of the engineering flows.

Separation induced transition

When a laminar boundary layer separate due to a too strong pressure gradient transition usually occurs because of the inviscid instability mechanics that takes places is the shear layer generated by the separation bubble and the free stream flow. This kind of transition usually occurs in presence of very intense pressure gradients such as in the rear part of a blunt body or on the rear part of the suction side surface of very highly loaded airfoils.

1.2 Transition in Turbomachinery

In the field of turbomachinery the study of the boundary layer plays a fundamental role. The developing of the turbulent structures in the boundary layer affect the local parameters such as skin friction and heat transfer coefficient. An example of the modification

of the local parameters: as represented in Fig.B.1 where is shown the distribution of the heat transfer coefficient along the pressure side and the suction side of a blade row and shows as in correspondence of the location of the transition the heat flux is enhanced. The strong modification of the local parameters can affect the global ones potentially causing a drop in the aerodynamic performances of the row and on the thermodynamic performances of the whole machine.

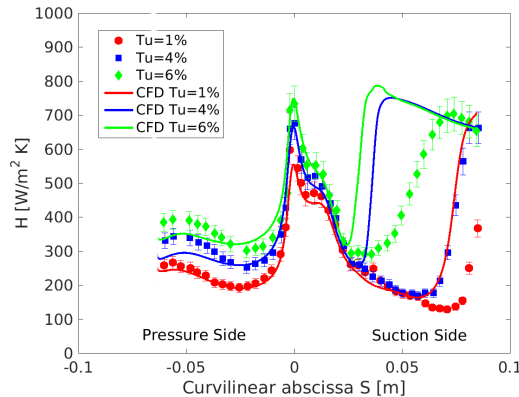


Figure 1.2: Heat Transfer Coefficient along the Pressure and Suction side of a nozzle guide vain

Due to the fact that the free stream conditions dictate the transition mode in a turbomachinery environment bypass and separation induced transition are the two modes more likely to occur. This is mainly due to the very high level of free stream disturbance such as high level of free stream turbulence intensity, free stream pressure gradient, wall curvature and surface roughness.

1.3 Outline of the project

After this very brief introduction is very easy to understand how the study of transition is a very challenging topic by itself and maybe even more if applied to a engineering flow such as the analysis of a turbomachinery component. The main aim of this project is to perform a numerical study of the bypass transition in a high loaded high pressure turbine inlet guide vane. The main tools of this work will be the state of art of the transitional models such as the $\gamma - Re_\theta$ [15, 19] by Menter and al. and the $k - k_l - \omega$ [28] by Walters and Cokljat integrated in a modern finite volume method RANS code. nowadays the use of this kind of transitional models is widely spread in CFD both in research and design practice, however these models aim to describe a very complex phenomenon with very few degrees of freedom. For these reasons they still strongly rely on a fine tuning of a certain number of empirical parameters according to well studied experimental observations on benchmark test cases. Usually this kind of models are tuned with quite simple test cases such as flow of flat plate in incompressible regime. This is the main

reason for which could be a quite interested topic test the thermal performances of these kind of models in a very demanding flow conditions such as the ones taking into account.

The report will be structured as follows:

- In chapter 2 will be presented a brief bibliographic review about the previous studies both experimental and numerical on the effect of the gas to wall temperature ratio on the transition.
- In chapter 3 will be introduced the theoretical framework and the basic idea behind the RANS transitional models exploited in this project
- The chapter 4 contains the main information about the numerical setup of the simulations, the grid independence and thermal validation
- In the chapter 5 the results coming from the simulation and the experimental results coming from a parallel experimental campaign on the same test case.
- In the last chapter will be discussed the most relevant results and will be proposed some hints for the next studies on the same topics.

Chapter 2

Bibliographic Review

In this chapter the most relevant results from the bibliographic review performed in the first part of the project will be briefly introduced. Moreover will be presented both the results from the experimental side and numerical side focusing our attention on the numerical results obtained so far.

2.1 Thermal effects on boundary layer

The laminar to turbulent transition is a very complex phenomenon involving a lot of tiny features of the flow, it is really challenging to be able to provide a fully description of the physics even for the simplest test cases. When other parameters, like the presence of a thermal field or strong pressure gradient, come into play the situation becomes even more complicated especially for simplified analysis technique such as correlation based approaches or RANS transitional models.

A very interesting work that can explain and justify the presence of some discrepancies between the measured results and the computed ones is the one of O. Sharma [26]. In particular some discrepancies between the prediction of the momentum and thermal transition length were found comparing the value of the heat transfer coefficient measured from experiment and the one computed by the classical turbulence transition models. The author suggests that this discrepancy could be due to fact that the value of the turbulent Prantl number Pr_T might present some functional dependency from the free stream pressure gradient. This concept is explained in Fig. 2.1 where three different pressure gradient distributions are represented. The left sketch shows how the evolution of the two boundary layers is similar in absence of relevant pressure gradient, in the central figure is shown that in presence of favourable pressure gradient the momentum boundary layer has a longer evolution respect to the thermal one, in the last figure on the left the opposite effect is shown. This result is particular relevant because in the RANS commercial codes the turbulent conductivity is related to the turbulent viscosity by mean of the turbulent Prandtl number assumed constant in all the flow field.

The work of Sharma [26] underlines how some basic assumptions commonly made in the RANS commercial codes about the characteristics of the flow could avoid to

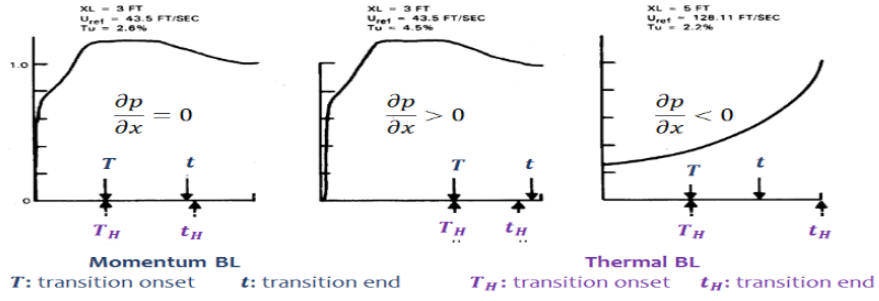


Figure 2.1: Influence of free stream pressure gradient on the turbulent Prandtl number [26]

describe in a proper way the evolution of the boundary layer in presence of strongly coupled momentum and thermal field and/or strong free stream pressure gradient.

2.2 Natural transition studies

In the previous chapter we explain some difficulties to describe the transition in presence of complex flow fields. Nevertheless could be useful to analyze some studies belonging to the field of Linear Stability Theory so only confined to natural transition. The basic idea of this approach is to consider the initial stage of the transition where the fluctuations are very small respect to the mean flow, this allows to linearize the equations and to reduce the N-S system to a linear algebraic system. This approach is very powerful and provide quite accurate predictions, however because of the hypothesis of small perturbation its results are reliable only in describing the inception of instability in a laminar flow and therefore it is limited to the study of natural transition. A very interesting work has been performed by Ozgen [21], he proposes to modify the Navier Stokes system for an incompressible flow in order to take into account the functional dependency of the thermo physical properties such as density and dynamic viscosity on the temperature. He found out that for gas flow, where the viscosity increase with the temperature, the increasing of heat transfer from the wall to the flow destabilize continuously the boundary layer, this can be seen in Fig. 2.2 noticing that the area inside the upper and lower branch reduces when the difference of temperature between the wall and the gas increases.

The physical explanation of this behaviour can be found in the analysis of the velocity profile in Fig 2.3

Analyzing Fig 2.3 can be seen that the presence of heat flux from the wall to the flow causes and increase in the velocity defect that usually means an increase in the value of momentum thickness and a continuous decrease of the critical Reynolds number. The heating modify both the viscosity and the density in opposite way so the final results will be a conjoint effect of both of them.

A similar technique was proposed by Shafer and Severin [24]. They were able to extend the classical stability theory for isothermal flow to non isothermal ones thanks to a Taylor

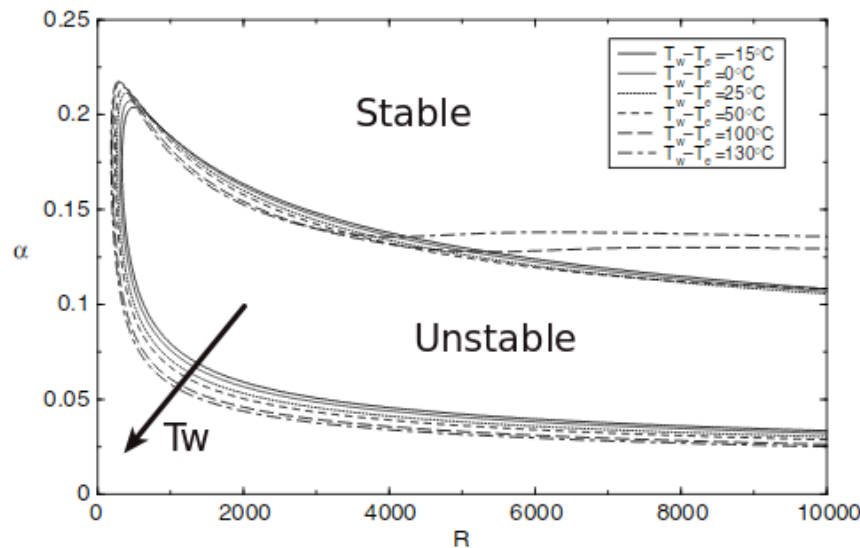


Figure 2.2: Stability region for incompressible and not isothermal boundary layer [21]

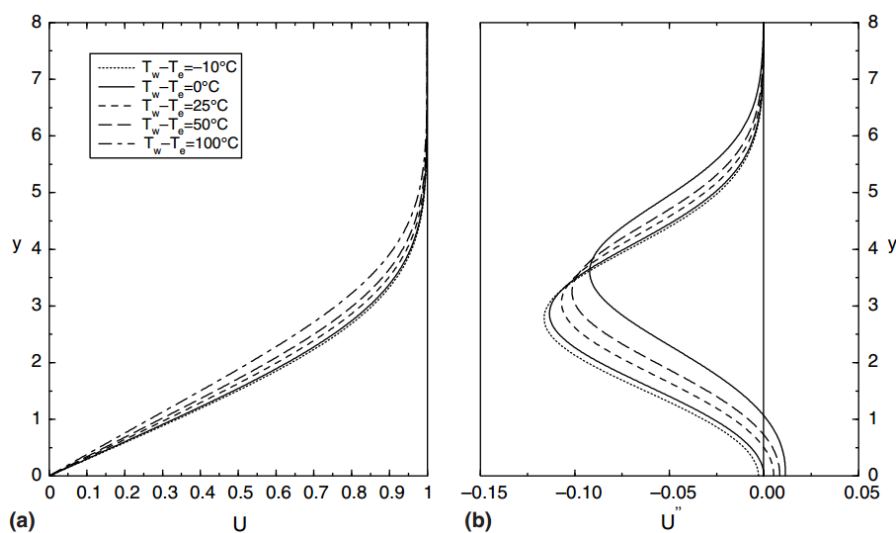


Figure 2.3: a) Velocity Profile b) curvature of Velocity profile [21]

expansion of the physical variables around a reference value. They found out that the linear stability of the boundary layer is modified by the heat transfer and in particular :

- Opposite stability behaviors for heating and cooling the flow.
- The effect is due to the variation of density and dynamic viscosity so only the variation of kinematic viscosity must be taken into account (this result is in agreement with the one of [21]).

The results obtained by in [21] [24] are particular interesting because both works are in quite good agreement with the conclusion drawn by [12]. They attribute the change of the stability properties to three physical effects:

- The change of the effective Reynolds number due to the change of the physical properties of the flow.
- The change of the velocity profile correlated with the change of the boundary layer integral parameters.
- The thin layer effect linked with the variations of the value of the viscosity very near the wall.

All this results are encouraging and show a quite clear trend, however it is important to stress that they are rigorously valid only in the framework of natural transition. It is still not clear if and how results can be extended to the bypass one where only few things are known.

2.3 Bypass transition studies

The bypass transition takes place when the level of environmental disturbance reaches a critical value [29]. Above this value the hypothesis of small perturbations above the mean flow is no more valid, so the linear stability theory discussed before is no more rigorously applicable.

In the literature there is a lack of studies about the effect of the temperature on the bypass transition. However from an experimental point of view an interesting work has been performed in the eighties by Sohn [27]. He attempted to characterize the bypass transition in a heated boundary layer measuring the characteristics of the thermal and momentum boundary layer. The result was that he observed an increase of the heat transfer due probably to the enhanced of low frequency modes in the spectrum. Another experimental study has been performed by Ferreira [10] at the von Karman Institute. The experimental campaign was carried out on a high pressure turbine transonic inlet guide vane. The idea was to measure the heat flux along the blade and from the time signal of the heat flux reconstruct the value of the intermittency function along the suction side of the blade as represented in Fig 2.4

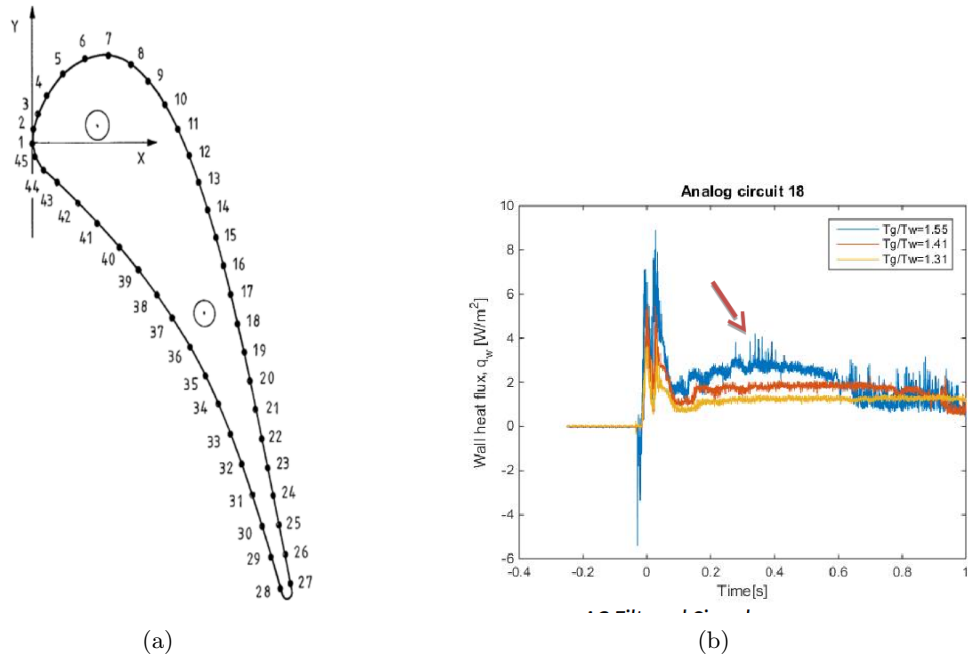


Figure 2.4: Location of the thin film and time resolved heat flux [10]

An increase in the fluctuation of the signal was observed while increasing the inlet total temperature, this can be considered a first empirical proof of a some kind of influence of the temperature ration on the bypass transition. Unfortunately during the experimental campaign she faced some issues to maintain the exit Mach number constant in the facility so it is not clear if these effects are due to the temperature ratio or to the variation of the Mach number. Another interesting experimental study is proposed by [7]. It seems to show that the variation of the ratio $\frac{T_b}{T_w}$ affects the turbulent spot production inside the boundary layer.

From a numerical point of view in the literature are present a lot of detailed analysis of the flow field inside a high pressure inlet guide vane. A detailed analysis has been performed by mean of a direct numerical simulation like in the work of [30] or LES simulations [20] ; the target of this studies wasn't to understand the effects of temperature but the complete characterization of the flow field and the effect of free stream turbulence intensity and length scale on the heat transfer and transition onset. A similar study has been performed by Morata [20] on the LS89 test case. A numerical analysis based on the optimal growth theory on the compressible boundary layer proposed by [4] seems to show that the cooling of the surface has a destabilizing effect on the boundary layer for higher subsonic Mach number and almost a negligible effect of the supersonic ones. In a quite recent work Maffulli [16] [23] found out that the predictions the RANS transitional models seem to be affected from the gas to wall temperature ratio. However it is not clear if this effect is physical or numerical and if the models are able to capture

the right physics of the phenomenon. In figure 2.5 is shown how the transition evolves differently for different temperature ratio (temperature ratio defined as $\frac{T_{w,all}}{T_0}$).

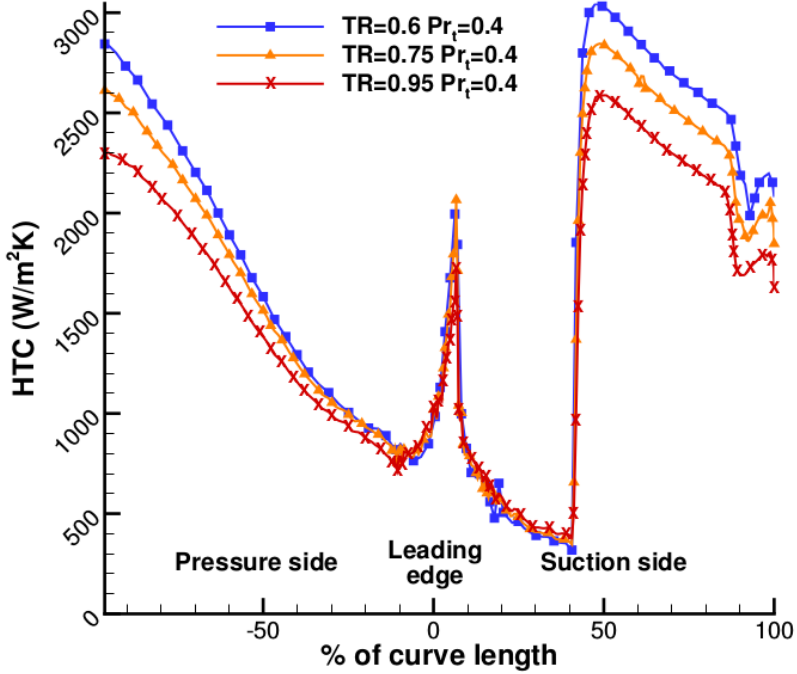


Figure 2.5: Heat transfer distribution for different temperature ratio [16]

An other interesting work is the article proposed by [8] in which a critical revision of the state of art transitional model for RANS code is performed. This paper provides an analysis of the performances of six different turbulence transition models embedded in N-S RANS code. The models tested start from the simplest ones based on correlation with the more complex single point one based on the laminar kinetic energy. All the models have been tested on well known test cases in adverse and favourable pressure gradient and in a well tested turbine cascade. As expected the result is that the transition onset correlations are not satisfactory in the complex case of the cascade test case and show the necessity to include the effects of free stream turbulence intensity in the laminar part of the boundary layer.

2.4 Conclusions

The most challenging part of this bibliographic review has been to find a general trend in the results and a widely used approach to study the effect of the temperature ratio on the bypass transition. Nevertheless it is worthy to report the most relevant results:

- The effect of the temperature on the natural transition seems clearly defined both

from an experimental point of view and for the framework of the linear stability theory[21].

- In The case of bypass transition the tool of linear stability theory is no more reliable so in order to perform numerical studies we need to go to high order method, that are to computational expensive, or RANS transition model, not validated for this operative conditions. The more relevant experimental works of [7] in which seems that the increase of $\frac{T_0}{T_w}$ has some effects on the turbulent spot productions.

Chapter 3

Transition Models

In this chapter will be explained the general idea behind the RANS transition models. Moreover the more technical and numerical details about the integration of the transition model with the existing turbulence model will be explained. Finally we will give a physical explanation of the parameters introduced in the model and try to understand why we will expect a certain kind of behaviour between a model and another.

3.1 General idea behind the RANS transition models

The basic idea of the RANS approach is to apply an average procedure to the governing equations in order to decouple the fluctuation and time dependent part of the flow from the mean and stationary one. Once applied this procedure on the N-S system only the mean part is resolved while the time depended one is modeled. In order to model the non resolved part of the flow additional equations have to be introduced (the so called turbulence model). The final result is a system composed by:

- Continuity
- Momentum equations
- Energy equation
- Turbulence Model

In the RANS average procedure all the time dependent feature of the flow field are lost, this doesn't allow the code to describe the inception and the amplification of the fluctuation that finally bring to the transition to turbulence. The basic idea in order to allow the model to be able to include in some way the effect of the transition to turbulence is to introduce auxiliary variables whose evolution can be correlated to the state of the boundary layer. Some useful guidelines in order to build this additional equations have been provided by Menter[19]:

- Allow the calibration of the predictions.

- Allow the description of the different transition mechanisms.
- Avoid multiple solutions.
- Do not modify the original turbulence model for the fully turbulent zone of the flow.
- Similar wall integration to the underlying turbulence model.
- Be coordinate system independent.
- Be applicable to three dimensional flows.

Nowadays two of the most promising approaches are the $\gamma - Re_\theta$ [19, 14] and the $k - k_l - \omega$ [28] of Walters and Cokljat.

- The basic idea of the $\gamma - Re_\theta$ is the introduction of two non physical quantities whose evolution can be correlated to the state of the boundary layer through empirical correlations. The advantage of this model is that it is easy to tune and very well tested on benchmark test cases, the major drawback is that it strongly relies on empiricism.
- The underlying idea of the $k - k_l - \omega$ is to add only one extra equation for the evolution the laminar kinetic energy. The laminar kinetic energy has the task to describe the evolution of the fluctuations in the pre-transitional boundary layer. In this case the transition is described as energy transfer between the laminar kinetic energy to the turbulent one. The main advantage of this model is that it relies on more physical consideration respect to the $\gamma - Re_\theta$, the drawback is that is still not widespread and diffused as the previous one.

3.2 $\gamma - Re_\theta$

The first model we take into consideration is the $\gamma - Re_\theta$ developed by Menter and Langtry [15]. The formulation proposed by this two authors is based on two additional transport equations, the first one, for the intermittency, controls the production of turbulent kinetic energy inside the boundary layer, the second, for the Re_θ , is introduced in order to include the influence of the free stream value of pressure gradient and turbulent intensity on the boundayr layer.

3.2.1 Vorticity Reynolds number as onset transition criterion

One of the biggest problems of the approach based on correlations, such as the model proposed by Abu Ghannam and Show [3], is that they rely on non local quantities such as momentum thickness (that comes from a line integration and therefore can't be defined locally). This is a serious drawback in fact it limits their application to two dimensional geometry and makes not possible to apply the model to unstructured meshes where the

variables are defined only in the cell centers. A smart way to overcome these limitations is to substitute the Reynolds number based on momentum thickness with the one based on the local value of vorticity defined as:

$$Re_v = \frac{d_{wall}^2 \Omega}{\nu} \quad (3.1)$$

It is easy to see how this definition of the Reynolds number depends only on local variable that can be easily computed in every cell center. From experimental observation [19] it comes out that the maximum of the profile of the Reynolds number based on the vorticity inside the boundary layer is proportional to the Reynolds number based on the momentum thickness up to an arbitrary constant according to the following expression.

$$Re_\theta = \frac{\max(Re_v)}{2.193} \quad (3.2)$$

It is important to underline that this relation changes according to the free stream pressure gradient; this features should be taken into consideration because the majority of cases in which the transitional model are calibrated fall into the region in which there is only a smaller change but this is not true in the flow every flow field of engineering interest.

3.2.2 Transport equation for Intermittency

The intermittency function γ is defined as the ratio between the time the flow present turbulent characteristic over the total time of observation according to the expression:

$$\gamma = \frac{\Delta t_{turb}}{\Delta t_{turb} + \Delta t_{lam}} \quad (3.3)$$

so we can directly correlate the value of the intermittency to the state of the boundary layer:

- $\gamma = 0 \rightarrow$ fully laminar flow
- $0 < \gamma < 1 \rightarrow$ transitional flow
- $\gamma = 1 \rightarrow$ fully turbulent flow

The transport equation for the intermittency reads:

$$\partial_t(\rho\gamma) + \partial_i(\rho U_i \gamma) = P_\gamma - E_\gamma + \partial_i((\mu + \frac{\mu_T}{\sigma}) \partial_i \gamma) \quad (3.4)$$

Where P_γ E_γ are the production and destruction term. For detailed description of all the terms we refer to the work of Menter and Langtry [14]. We focus only our attention on the production term that has the following form:

$$P_\gamma = F_{length} c_{a1} \rho S [\gamma F_{onset}]^{0.5} (1 - c_{a1} \gamma) \quad (3.5)$$

Inside the production term P_γ we can identify the following terms:

- $ca1$ is a constant of the model.
- S is the norm of the strain tensor.
- F_{length} is an empirical correlation that define the transition length, it is based on the value of the momentum thickness Reynolds number in the free stream.
- F_{onset} is the correlation that regulates the onset of the transition.

The main objective of this work is to study the effect of the temperature on the transition location, for this reason we focus our attention of the expression of F_{onset} defined as :

$$F_{onset} \sim \frac{R_v}{2.193R_{\theta c}} \quad (3.6)$$

where R_v is the vorticity Reynolds number previously introduced and $R_{\theta c}$ is the critical Reynolds number where the intermittency start to grow inside the boundary layer, in other words it can be seen as the location where the turbulence fluctuations starts to increase. Its value is obtained from an empirical correlation based on the value of $\tilde{R}_{\theta t}$ transported by the second equation of the model. This terms is used to trigger the itermittency production an will be one of the central object of our analysis.

3.2.3 Transport equation for the transition momentum thickness Reynolds number

As said before the this kind of model strongly relies on empirical correlations in particular the Reynolds number of transition onset $Re_{\theta t}$ is defined as a function of the free stream values of FSTI and pressure gradient $\frac{dp}{ds}$:

$$Re_{\theta t} = f(Tu, \frac{dp}{ds}) \quad (3.7)$$

It is noteworthy to observe that the value of $Re_{\theta t}$ is required by the intermittency equation inside the boundary layer. Moreover the variables like turbulence intensity Tu and the pressure gradient $\frac{dp}{ds}$ change significantly through the domain especially for flow with non negligible pressure gradient such as the transonic blades rows. Since one of the fundamental request of the model is that only local quantities are treated we introduce a new variable \tilde{Re}_t that is transported all over the whole domain. The two basic ideas of this approach are the followings:

- We treat the transition momentum thickness Reynolds as a transported scalar quantity
- Then we use empirical correlations to compute the \tilde{Re} in the free stream and we allow the value of the free stream to diffuse into the boundary layer.

The transport equation for the momentum thickness transition Reynolds number is defined as follows:

$$\partial_t(\rho \tilde{Re}_{\theta t}) + \partial_i(\rho U_i \tilde{Re}_{\theta t}) = P_{\theta t} + \partial_i(\sigma(\mu + \mu_T)_i \tilde{Re}_{\theta t}) \quad (3.8)$$

Where the source term is defined as :

$$P_{\theta t} = c_{\theta t} \frac{\rho}{t} (Re_{\theta t} - \tilde{Re}_{\theta t})(1 - F_{\theta t}) \quad (3.9)$$

$P_{\theta t}$ is defined in such a way that outside the boundary layer the value of $\tilde{Re}_{\theta t}$ is forced to be equal to the value of $Re_{\theta t}$ compute with empirical correlations as a function of Tu and $\frac{dp}{ds}$.

3.2.4 Coupling with existing turbulence model

In this section we briefly explain how the transition model is coupled with the turbulence model. The recommended turbulence is the $k - \omega - SST$ for further details we refer to [18]. The modified equation are the following:

$$\partial_t(\rho k) + \partial_i(\rho U_i k) = \tilde{P}_k - \tilde{D}_k + \partial_i((\mu + \sigma \mu_T)_i k) \quad (3.10)$$

$$\partial_t(\rho \omega) + \partial_i(\rho U_i \omega) = \alpha \frac{P_\omega}{\nu_T} - D_\omega + \partial_i((\mu + \sigma \mu_T) \partial_i \omega) \quad (3.11)$$

where $\tilde{P}_k \sim \gamma P_k$ and $\tilde{D}_k \sim \gamma D_k$ are the modified source and destruction terms introduced in order to take into account the growth of turbulent kinetic energy in the transitional boundary layer.

3.3 $k - k_l - \omega$

The second model analyzed is the model based on the laminar kinetic energy concept developed by Walter and Cokljat [28]. The basic idea is to introduce in the existing turbulence model, the $k - \omega SST$ [18] in this case, a third transport equation for a new variable k_l . The laminar kinetic energy k_l represents the energy content of the non turbulent stream wise fluctuations in the pre-transitional boundary layer. Unlike the $\gamma - Re_\theta$ the closure of this model is based on a more physics based observations rather than a purely empirical approach. Moreover the introduction of a local quantities such as the laminar kinetic energy k_l and a phenomenological approach make the model local, and for this reason easy to integrate in a modern CFD solver.

3.3.1 Phenomenology of transition

Despite the real physics underlying the transition process is not still completely understood recent numerical and experimental results have helped to underling some of the relevant features involved in the transition process. For low free stream turbulence

intensity the development and self-amplification of low amplitude velocity fluctuations (Tollmein Schlichting waves [25]) has been observed. As the free stream disturbance grows the velocity profile of the pre transitional boundary layer becomes more and more distorted. This distortion is accompanied by the development of a stream wise velocity fluctuations, this process leads to an increase of heat transfer and skin friction and can eventually bring to turbulence generated by a breakdown of these structures (called Klebanoff modes [29], [22]).

The main target of the introduction of the laminar kinetic energy is to describe the development of pre-transitional fluctuations that can eventually lead to transition to turbulence. Although the dynamic of the transitional fluctuation is not entirely understood however the author[28] underlines how two aspects are critical:

- The selectivity of the boundary layer: the frequency content of k_l seems to be universal and relatively independent from the spectrum of the external forcing.
- The dynamic of the growth of k_l inside the boundary layer has found to be quite universal and in particular the energy growth is proportional to Re_x , where x is the distance from the trailing edge.

These observations suggests that this kind of modelling approach based on the appropriate parameters may be able to describe the right behaviour of the transitional boundary layer.

From the model point of view the transition is represented as a energy redistribution from the large scale [22] (represented by k_l) to the small scale (represented by k_T) and not as a turbulent energy production. The onset on transition is decided on local condition (the locality of the model is preserved). The author [28] proposes that the most important parameter in order to trigger the transition is the ratio between the turbulent production time scale and the molecular diffusion time scale; when this ratio reaches a critical value the transition is triggered. It is important to stress that this criterion is valid for both natural and bypass transition [28], we only need to change the definition of time scale.

3.3.2 Model formulation

As explained in the previous sections the philosophy of the RANS transition model is to add to an existing N-S solver extra transport equations in order to try to model the behaviour of the transitional boundary layer. The $k - k_l - \omega$ model is composed by the $k - \omega - SST$ turbulence model integrated with an additional transport equation that describes the evolution of k_l . The mathematical formulation of the model for compressible flows is the following:

$$\partial_t(\rho k_T) + i (\rho U_i k_T) = \rho(P_{k_T} + R_{BP} + R_{NAT} - \omega k_T - D_T) + \partial_i((\mu + \frac{\rho \alpha_T}{\sigma_k}) \partial_i k_T) \quad (3.12)$$

$$\partial_t(\rho k_l) +_i (\rho U_i k_l) = \rho(P_{k_l} - R_{BP} - R_{NAT} - D_l) + \partial_i(\mu \partial_i k_l) \quad (3.13)$$

$$\begin{aligned} \partial_t(\rho \omega) + \partial_i(\rho U_i \omega) &= \rho(C_{\omega 1} \frac{\omega}{k_T} P_{k_T} + (\frac{C_{\omega R}}{f_W}) \frac{\omega}{T} (R_{BP} + R_{NAT}) - C_{\omega 2} \omega^2 \\ &\quad + C_{\omega 3} f_{\omega} \alpha_T f_W \frac{\sqrt{(k_T)}}{d^3}) + \partial_i(\mu + \frac{\rho \alpha_T}{\sigma_k}) \partial_i \omega \end{aligned} \quad (3.14)$$

For a detailed explanation of the terms inside the equations we refer to the paper of [28]. Here we will analyze only the terms directly involved in the energy transfer responsible of the onset of the transition process.

The terms in the right hand side of the equations that have the task to transfer energy from the bigger length scale to the smaller ones are the following : R_{BP} and R_{NAT} ; the first term has the role to describe the bypass transition the second one the natural one. It is interesting to notice the sign of this two terms : they have the minus sign in the equation for the laminar kinetic energy and the plus sign in the equation for the turbulent kinetic energy. This allows the model to describe the transition as energy transfer between the large scales (laminar part) to the small ones (turbulent part). All the details are provided in the paper of [28], here we consider only the term concerning the bypass transition.

As explained before the basic idea of this model is to model transition as an energy transfer between the large and small scale, the term representing the bypass transition is the following:

$$R_{BP} = C_R \beta_{BP} k_l \frac{\omega}{f_W} \quad (3.15)$$

The onset of transition is regulated by the threshold function:

$$\beta_{BP} = 1 - e^{-\frac{\phi_{BP}}{A_{BP}}} \quad (3.16)$$

$$\phi_{BP} = \max[\frac{k_T}{\nu \Omega} - C_{BPcrit}, 0] \quad (3.17)$$

The non dimensional group of quantities $\frac{k_T}{\nu \Omega}$ represents the ratio between the turbulent production time scale and the viscous dissipation time scale while C_{BPcrit} is a constant of the model that represent the critical value of $\frac{k_T}{\nu \Omega}$ above whose the energy transfer begins.

The basic behaviour of the model can be summarized in the following way:

- The model transport the two quantities k_l and k_T , they evolve separately once the critical value of $\frac{k_T}{\nu \Omega}$ is reached.

- Once the critical value of $\frac{k_T}{\nu\Omega}$ is reached the function ϕ_{BP} becomes different from zero and as consequences also β_{BP} becomes different from zero. This switch on the term R_{BP} that initiates the transfer of energy from the large scale (laminar part) to the smaller scale (turbulent part). The beginning of the energy transfer can be seen as the onset of the transition.

3.4 Final remarks

After this brief introduction about the general idea underlying the RANS transitional models it is important to stress out that these models are very attractive because of the low computational effort needed and because of nowadays they are widely validated on benchmark test case. However the real physics of transition is still not well understood and this is the main reason for which this model have still to rely on empirical correlations. The correlation used are very well tested for benchmark cases however we have to be very careful to use them for more naive computation.

Finally it is important to underline that the main target of this project is not to study the physics of the phenomenon through the transition models but to understand the limit of them and to try to understand the possible way to extend their application to more and more demanding test cases.

Chapter 4

Numerical set up and Validation

In this chapter we will present first the numerical set up of the simulations: numerical technique adopted, the computational domain and the properties of the mesh. In the last part of the chapter we will present the grid independence and the first numerical validation against experimental results from the literature.

4.1 Space discretization

The governing equations have been discretized by means of a finite volume method code on an structured and unstructured mesh. Nowadays a lot of numerical techniques are available in order to solve the balance equations, such as finite elements finite differences and finite volumes. In this work the finite volumes technique has been chosen for its ability to handle with discontinuous flow features of the flow in a compressible regime such as shock waves. The governing equations can be rearranged in the following form:

$$\frac{\partial U}{\partial t} + \frac{\partial(F - F_v)}{\partial z} + \frac{\partial(G - G_v)}{\partial y} = S \quad (4.1)$$

where U is the vector of the conservative variables F F_v the inviscid and viscous flux along the axial direction, G G_v the inviscid and viscous flu along the radial direction and S is the vector that include all the source terms.

The finite volume technique involves the integration of the balance equations on an elementary control volume. This yields to:

$$\int_V \frac{\partial U}{\partial t} dV + \int_V \left(\frac{\partial(F - F_v)}{\partial z} + \frac{\partial(G - G_v)}{\partial y} \right) dV = \int_V S dV \quad (4.2)$$

Thanks to the Gauss-Green theorem we can rearrange this expression as:

$$\int_V \frac{\partial U}{\partial t} dV + \int_{\partial V} ((F - F_v)n_z + (G - G_v)n_y) d\Sigma = \int_V S dV \quad (4.3)$$

The convective and diffusive flux can be computed as a summation of the contributions over all discrete faces bounding the elementary control volume. This assumption leads to:

$$\frac{\partial U}{\partial t} = \frac{1}{V} \sum_{j=1}^{N_j} E_j \Sigma_j + S \quad (4.4)$$

where E is a symbolic notation to indicate the totality of flux across the boundary faces.

The space discretization exploited are: second order central scheme for the computations performed with the FINE Turbo solver and second order upwind for the computations performed with the ANSYS Fluent solver.

4.2 Time discretization

The system of equations are solved under their unsteady form despite the fact that only the steady solution is of interest. This method is so called time marching method and has been developed in order to avoid the difficulties linked to compressibility effects. In this work a 4 stages explicit Runge Kutta scheme has been used, the more general for a multistage method for the equation:

$$\frac{\partial U}{\partial t} = F(U) \quad (4.5)$$

$$U^1 = U^n + \alpha_1 \Delta t F(U^N)$$

$$U^2 = U^n + \alpha_2 \Delta t F(U^1)$$

$$U^q = U^n + \alpha_q \Delta t F(U^{q-1})$$

$$U^{n+1} = U^q$$

The coefficients α_i determine the stability area. Cause the explicit method is conditionally stable the temporal and spatial parameters must satisfy the following relation.

$$\left| \lambda_{max} \frac{\Delta t}{\Delta x} \right| < \nu_{max} \quad (4.6)$$

Where the ν_{max} is the maximum allowable Courant's number (function of the parameters of the scheme) and λ_{max} is the max eigenvalues of the Jacobian matrix of the fluxes.

4.3 Mesh and computational domain

The computational domain is sketched in Fig 4.1. The mesh was created with NUMECA Autogrid it is a structured mesh with a multi-block approach and a 4H-O topology. The 4H-O topology is made by an O-block that wraps around the profile and 4 H-blocks in order to define the geometry of the channel. This topology has been chosen in order to preserve a good orthogonality between the wall and the first cells inside the boundary layer and to avoid too high skeweness for the cell near the periodic connections. More detailed information can be found in the User manual of NUMECA [2]. The inlet has been collocated one chord upstream the leading edge and the outlet 1,5 chord downstream the trailing edge in order to limit as much as possible the dependency of the solution from the position of the outlet boundary. The boundary conditions for the computation domain are isothermal wall for the pressure and suction surface of the profile, periodic conditions on the top and bottom boundary and subsonic inlet and outlet.

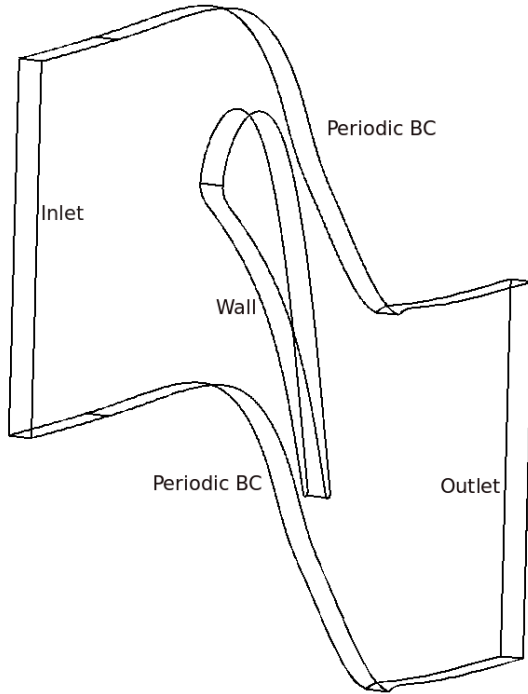


Figure 4.1: Computational Domain around the profile

4.3.1 $\gamma - Re_\theta$ grid independence

A first grid independence has been performed with the $\gamma - Re_\theta$ model. The grid independence has been reached on a mesh, represented in Fig 4.2 of around 200.000 elements. The value of $y+$ in the first cell center near the wall has been kept lower than 1 in order

to be able to compute the flow features of the boundary layer [6]. The expansion ratio of the cells near the wall was kept lower than 1.1 and the condition of non matching periodicity is imposed in order to avoid cell with a too high skewness near the periodic connections. Some particulars of the mesh at TE and on the periodicity connection are reported in Fig A.1

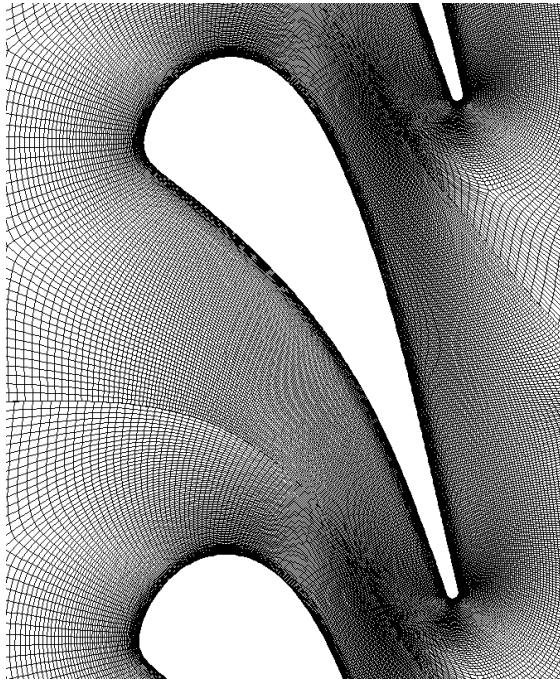


Figure 4.2: Mesh

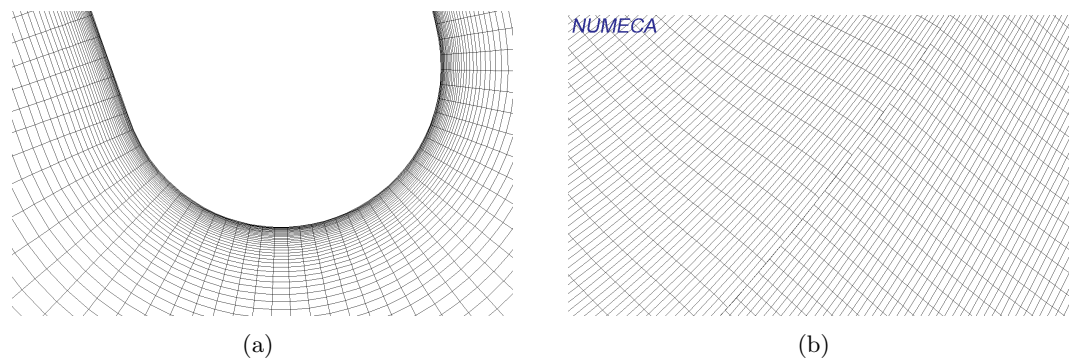


Figure 4.3: Details at TE a) and of the periodic connections b)

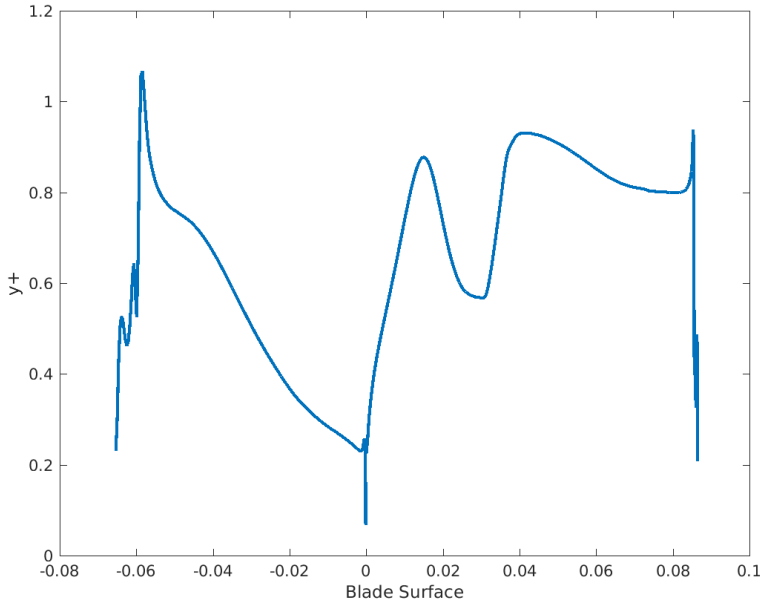


Figure 4.4: Distribution along the blade PS and SS

4.4 Aerodynamic and thermal validation

After the mesh has been generated a grid sensitivity analysis has been performed. The sensitivity analysis has been performed on the value of the heat transfer coefficient H defined as $H = \frac{q_w}{T_w - T_0}$. We choose this parameters because its absolute value is very sensitive to the number of cells in the boundary layer. Moreover its trend along the suction side shows the onset and the evolution of the transition and furthermore the location of the transition is very sensitive to the number of points in the stream wise direction. For these reasons we have considered the grid independence to be reached when we observe no modifications in absolute value of the heat transfer coefficient and moreover there are no more modifications in the location of the transition as showed in Fig 4.5. The boundary conditions come from the experimental campaign of Arts[5] and Fontaneto [11] on the same test case.

$T_0[k]$	M_{2is}	Re_{2is}	T_u	$L_t[m]$	T_{ratio}
408	0.7	10^6	1% - 6%	0.02	1.36

Table 4.1: Boundary conditions for the thermal validation of the $\gamma - Re_\theta$ measured by [5]

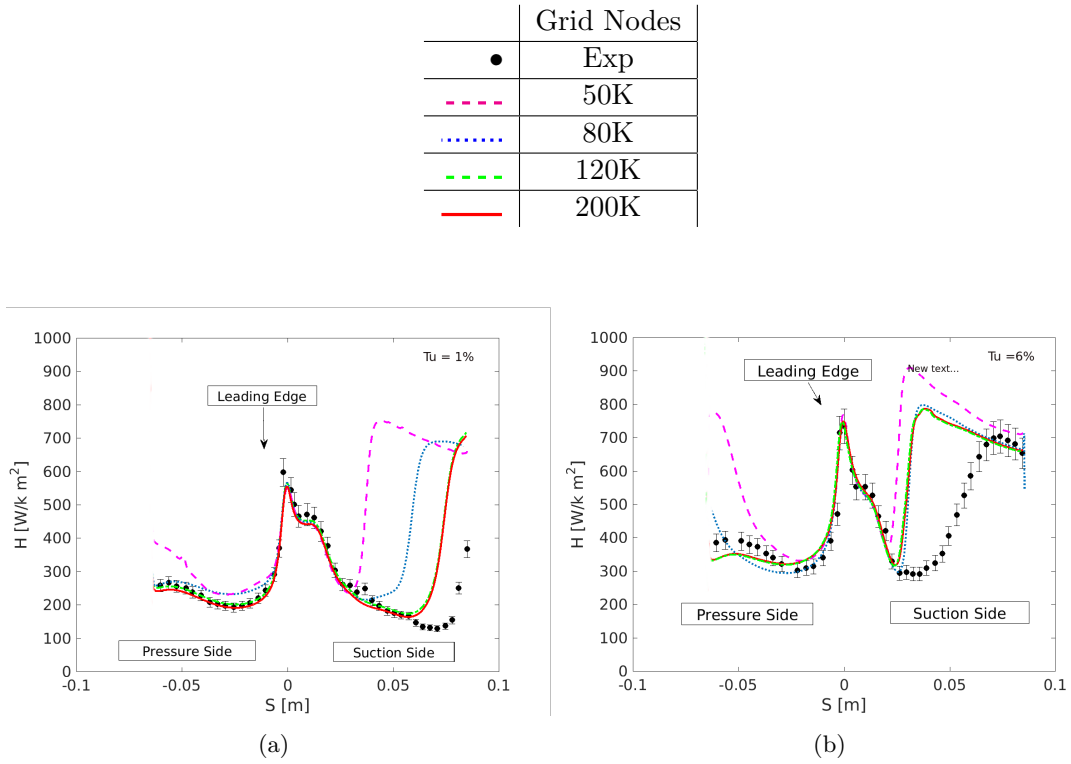


Figure 4.5: Distribution of the heat transfer coefficient for two different value of free stream turbulence intensity $Tu=1\%$ and 6% .

The results once reach the grid independence have been compared to the experimental results obtained by Arts [5] in order to check that at least in the fully laminar and fully turbulent part of the boundary layer the codes predicts the right value of the heat transfer coefficient.

Finally once reached the grid independence and performed a first thermal validation we have made a comparison between the value of the isoentropic mach number computed by the code and measure by the experiments of Arts [5] in order to obtain a further aerodynamic validation of the code. The results are reported in fig 4.6; we choose two value of isoentropic mach number: lower subsonic and high subsonic. The boundary condition for the computation are the following:

$T_0[K]$	M_{2is}	Re_{2is}	Tu	$L_t[m]$	T_{ratio}
408	0.84-1.02	$10^6 \cdot 10^5$	0.8	0.02	1.36

Table 4.2: Boundary conditions for the aerodynamic validation of the $\gamma - Re_\theta$ for comparison with [5]

●	EXP
—	CFD

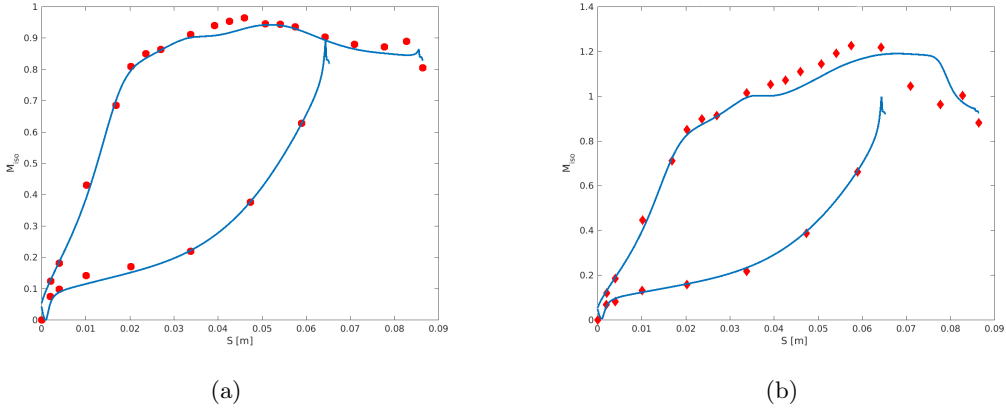


Figure 4.6: Isoentropic Mach number distribution

4.4.1 $k - k_{l-\omega}$ grid independence

After having reached the grid independence with the $\gamma - Re_\theta$ model we have performed a similar analysis with the $k - k_l - \omega$. Three different grids have been generated in NUMECA Autogrid and imported in Fluent. In order to be usable by fluent the structured meshes generated by Autogrid need to be declared as unstructured. The same procedure has been applied for the computation with the $k - k_l - \omega$, the distribution of the H coefficient along the blade surface is reported in figure 4.7. The boundary conditions for the computations reported in the following table, are the followings:

$T_0[k]$	M_{2is}	Re_{2is}	Tu	$L_t[m]$	T_{ratio}
408	0.7	10^6	6%	0.02	1.36

Table 4.3: Boundary conditions for the thermal validation of $k - k_{l-\omega}$ computation, measurement from [5]

4.5 Remarks

This chapter has been dedicated to the explanation of the numerical technique that will be exploited during our analysis. The grid independence was reached on a grid of around 200K elements, for both $\gamma - Re_\theta$ and $k - k_l - \omega$, paying attention to keep the value of $y+$ in the first cell near the wall always below one. The first validation against the experimental results show how both codes are able to retrieve quite accurately the value of isoentropic Mach number confirming a good prediction of the aerodynamic performances of the cascade. About the heat transfer coefficient it is noteworthy to underline how the code is in good agreement with the experimental results for both the $\gamma - Re_\theta$ and for the $k - k_l - \omega$ for the fully laminar (where the turbulence model is off) and for the fully

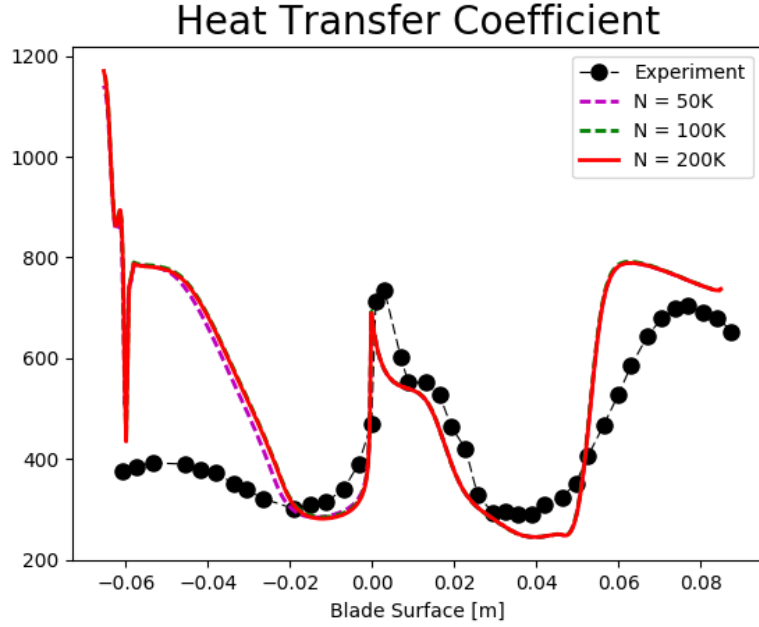


Figure 4.7: $k - k_l - \omega$

turbulent part. However the location and the length of development of the transition is not always well predicted. This behaviour is quite in agreement with some other computations on complex geometries found in literature. It is quite reasonable find this kind of behaviour because the transition area is where the more complex phenomenon take place and where the approximations of the model are stronger.

Chapter 5

Results

In this chapter the main results of this work will be presented. We have conducted two simulation campaigns with two different transition model, one with the $k - k_l - \omega$ and the other one with $\gamma - Re_\theta$. The simulation campaigns have been conducted on the LS89 profile, the VKI transonic cascade. The main target of the numerical campaign is to understand how the predictions of the two transitional model taken into considerations change varying the temperature ratio. The temperature ratio in this work has been defined as the ratio between the free stream total temperature and the wall temperature $T_{ratio} = \frac{T_0}{T_{wall}}$. Then the computations have been compared with the experimental results, the experimental results have been obtained keeping the wall temperature constant and varying the free stream condition. However numerically there is also an other way to reach similar working conditions: to keep the free stream constant and vary the wall temperature. Here both approaches have been performed in order to test the internal coherency of the model.

5.1 Preliminary aerodynamic study

Some works from the literature such as [20] [22] and from previous studies performed by Arts [5] that the transition is mainly influenced by three parameters:

- The Free Stream Turbulence Intensity $FSTI$
- The Reynolds Number Re
- The Free Stream Pressure Gradient $\lambda \sim \frac{1}{U_\infty} \frac{dU_\infty}{ds}$

There are also other parameters that play a secondary role such as : the temperature, the wall roughness, the noise.... In order to be able to observe the effect of the temperature on the transition both experimentally than numerically we have to exclude the influence of the main parameters that could overcome the ones of secondary strength. Five simulations have been performed at different value of exit isoentropic mach number M_{2iso} : from 0.5 up to 0.9.

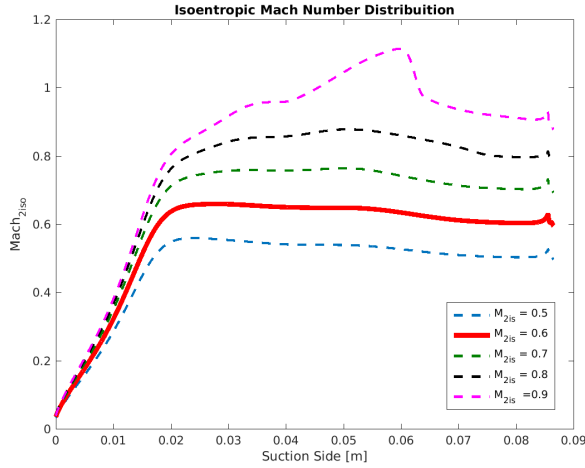


Figure 5.1: Isoentropic Mach Number distribution at different value of M_{2iso}

The results reported in Fig 5.1 shown how for too high exit mach number (above 0.8-0.9) the velocity distribution present strong pressure gradients that can overcome the effect of the temperature and leads the onset of the transition. However for too low exit Mach number (values below 0.5) we could loose the compressibility effects, loosing the compressibility effect means to loose the coupling between the thermal and momentum field that is one of the interesting features of this study. Because one of the target of this work is to perform an evaluations of the capabilities of the RANS transition models applied to the turbomachinery flows we choose to operate with a Mach number in between the value of 0.5 and 0.6 in order to maintain compressiblity and avoid to strong pressure gradients.

5.2 Experimental results at low turbulence intensity

The experiments and the simulations has been performed imposing as boundary conditions the value of:

- Inlet Total Temperature T_0 for the simulation with constant free stream and wall temperature T_{wall} for the simulation with constant wall temperature.
- Outlet Isoentropic Reynolds Number Re_{2iso}
- Outlet Isoentropic Mach number M_{2iso}
- Free Stream turbulence Intensity $FSTI$ and turbulence integral lenght scale L_t
- Temperature ratio defined as $T_{ratio} = \frac{T_0}{T_{wall}}$

Experimentally the transition is localized trough the value of the heat transfer coefficient $H = \frac{q_w}{T_w - T_0}$. From the heat transfer coefficient distribution is easy to understand

the approximate location of the transition. The simulation has been performed with the following boundary conditions:

$T_{wall}[K]$	M_{2is}	Re_{2is}	T_u	$L_t[m]$	T_{ratio}
294	0.55	$9.5 \cdot 10^5$	0.8	0.02	1.18-1.38-1.53

Table 5.1: Boundary condition measured in the facility for the case at low turbulence intensity and low $FSTI$

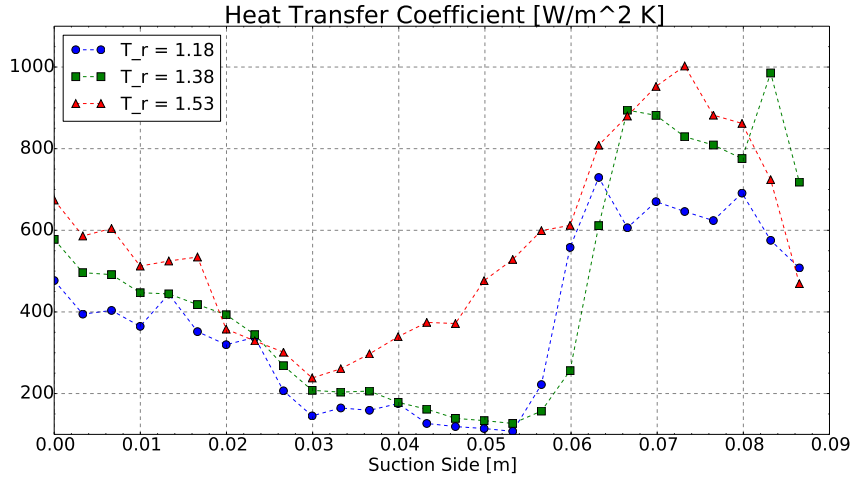


Figure 5.2: Heat Transfer Coefficient From the Experiments

From the experiments a clear trend emerges, in particular the results is that increasing the temperature ratio destabilizes the flow leading to an earlier transition. Moreover the effect seems not to be continuous but to have a certain threshold value below which the instability start to grow . In fact for the temperature ratio ($\frac{T_0}{T_{wall}}$) equal to 1.18 and 1.38 the transition point doesn't move appreciably. However when we go to the next temperature ratio 1.53 there is a huge shift of the location transition.

5.3 $\gamma - Re_\theta$ with $T_{wall} = 294[K]$

The first simulation campaign has been performed with the $\gamma - Re_\theta$. The boundary conditions applied are:

$T_{wall}[K]$	M_{2is}	Re_{2is}	T_u	$L_t[m]$	T_{ratio}
294	0.55	$9.5 \cdot 10^5$	0.8	0.02	1.18-1.38-1.53

Table 5.2: Boundary conditions for the $\gamma - Re_\theta$ at wall temperature constant and low $FSTI$

In this case we impose the right temperature ratio keeping the temperature of the blade constant and varying the free stream. The results obtained for the heat transfer coefficient along the blade are reported in Fig 5.3

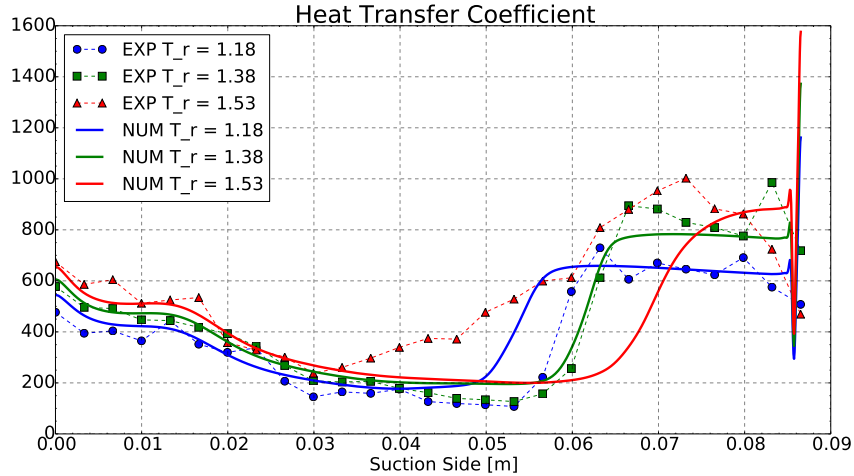


Figure 5.3: Heat Transfer Coefficient From the Experiments

The model seems to see an effect of the temperature on the transition, however the trend is the opposite respect to the experimental results. In fact the increase of temperature ratio and of the wall heat flux from the flow to the blade seems to stabilize the flow moving the transition downstream instead of destabilize it as shown from the experiments. In order to try to explain the behaviour of the model six normal cuts Fig. 5.4 to the surface of the blade has been performed in order to understand the influence of the temperature ratio on the kinematic, physical and turbulent quantities and try to justify the behaviour of the transition model. The location of the cuts along the suction side are reported in the following table:

Section	1	2	3	4	5	6
Location % of SS	6	23	47	58	70	82

Table 5.3: Locations in the percentage on the suction side of the cuts' location

Then the more relevant kinematic, turbulent and physical quantities have been plotted in order to understand the differences in their evolution. In the following figures the y axis represents the distance from the wall divided by the value of the local thickness of the boundary layer. On the x axis is reported the value of the analyzed quantities divided with the respective free stream value in the case of a dimensional variable.

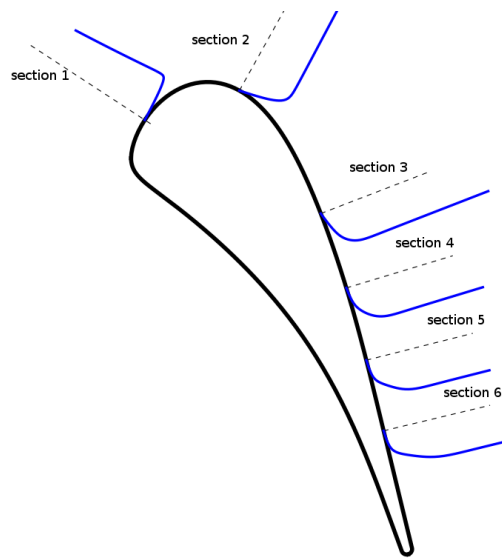


Figure 5.4: Location of the cuts

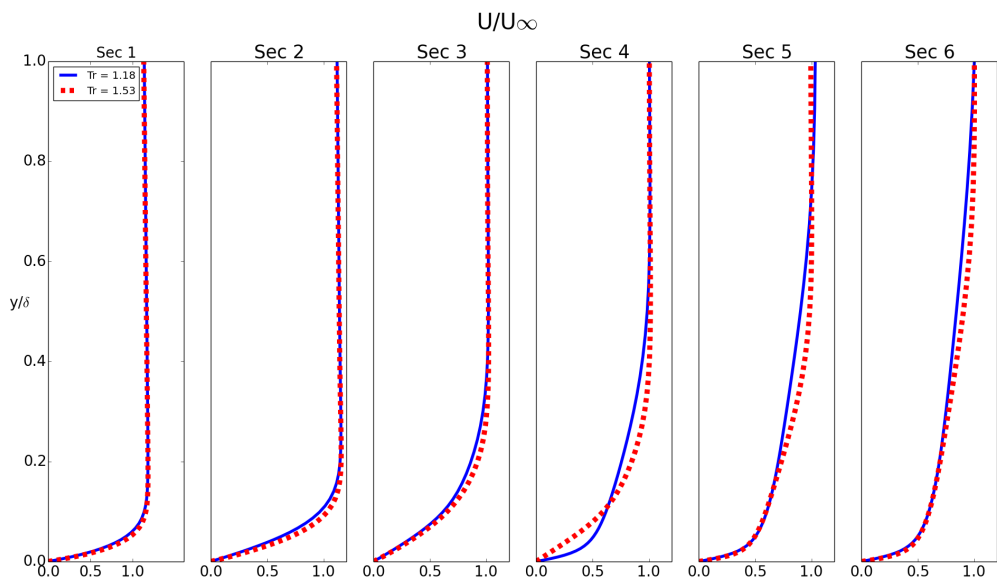


Figure 5.5: Absolute Velocity

5.3.1 Velocity profile

From the above distribution 5.5 is possible to notice how because of the compressibility effects that couple strongly the kinematic and thermal field already in the laminar part

(section 1,2,3) some differences in the shape of the profile emerge, in the section four the profile shape changes because the case with lower temperature ratio has already reached transition while the other one not. In the turbulent part it is possible to observe a slightly difference of the velocity profiles, this could be mainly due to the fact that a different transition location leads to a different evolution of the turbulent quantities and to a different evolution of turbulent viscosity that finally affects the shape of the velocity profile.

5.3.2 Density and viscosity

As explained in the Chapter 3 one of the variable that trigger the onset of the transition is the local vorticity Reynolds number defined as $Re_v = \frac{\rho g^2 \Omega}{\mu}$. The physical quantities depending on the temperature involved in this criterion are the density and the dynamic viscosity of the fluid.

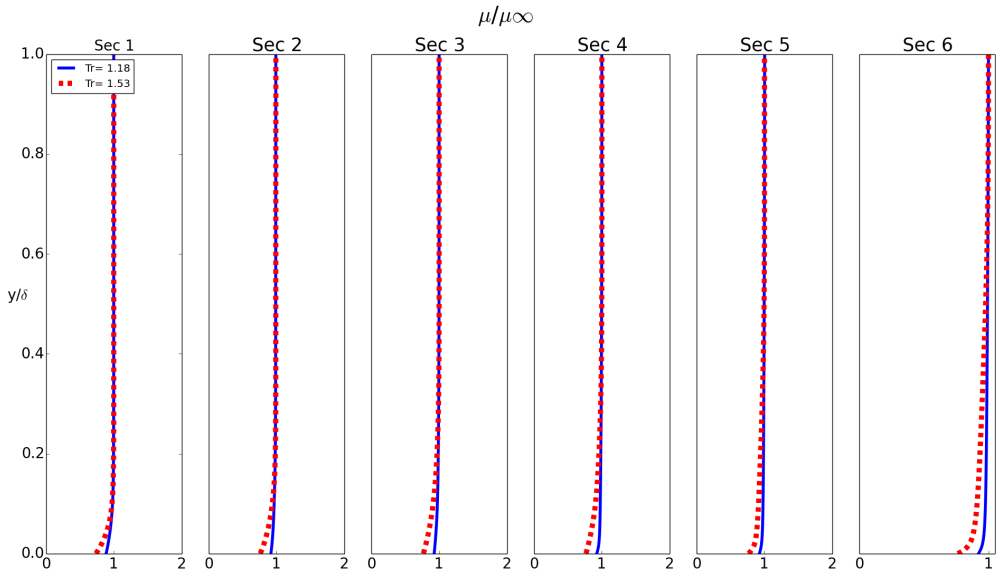


Figure 5.6: Dynamic Viscosity

As plotted in Fig 5.6 increasing the temperature the dynamic viscosity increases according to the Sutherland Law while the density decrease according to the perfect gas law. It is important to stress that all the quantities are related to the free stream value; so increasing the temperature ratio is equivalent to increase the temperature of the free stream and this correspond to make the difference between the value at the wall and the value outside the boundary layer greater.

As proposed by some author [24] in the study of the natural transition, because of the fact that the stability of the boundary layer depends both on the variation of density and dynamic viscosity could be convenient to study the stability in terms of the kinematic

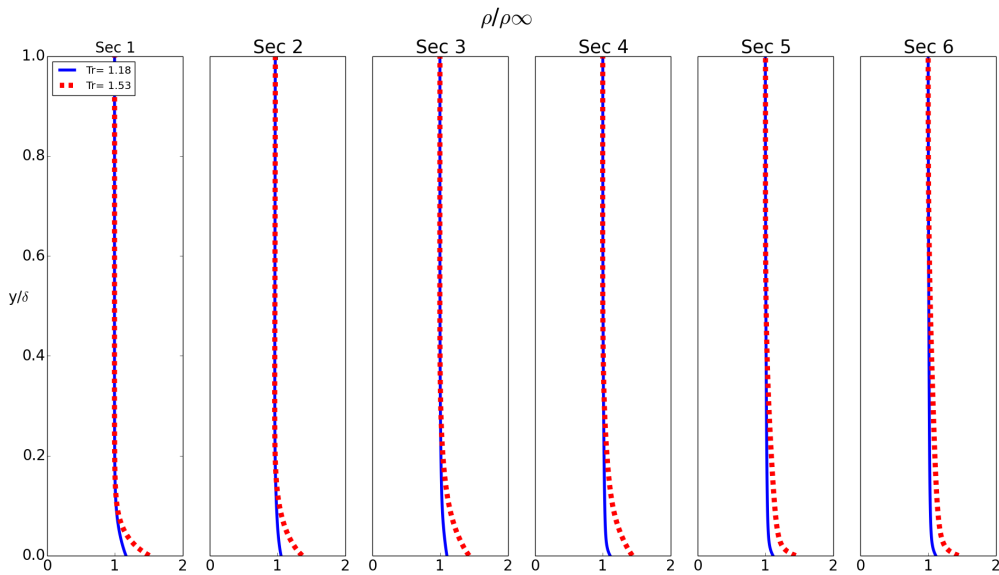


Figure 5.7: Density

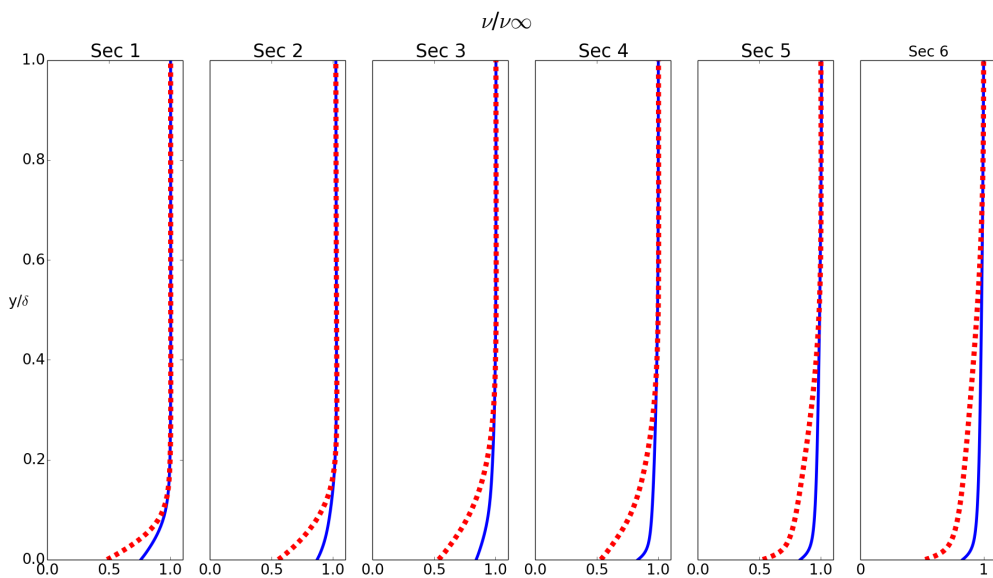


Figure 5.8: Kinematic Viscosity

viscosity defined as the ratio of the two precedent quantities $\nu = \frac{\mu}{\rho}$. From the Fig. 5.8 it is possible to see how the conjoint effect of the decrease of viscosity and increase of density produces a appreciable variation of kinematic viscosity near the wall. This effect

must be taken into consideration because of the dependency of F_{onset} from the value of these parameters.

5.3.3 Turbulent quantities

Finally the last quantities we have to take into consideration are the variables transported from the turbulence transition model. We recall that the intermittency is the variable that regulated the laminar (if equal to 0) or turbulent state (if equal to 1) of the boundary layer. From the distribution of the intermittency (Fig 5.9) inside the boundary layer it is easy to understand the state of the boundary layer. In particular we can see how in the first two sections the boundary layer is still laminar in both cases. In the third and fourth the transition takes places before for the lower temperature ratio modifying the shape of the profile. Finally the last two cuts the boundary layer is fully turbulent in both cases.

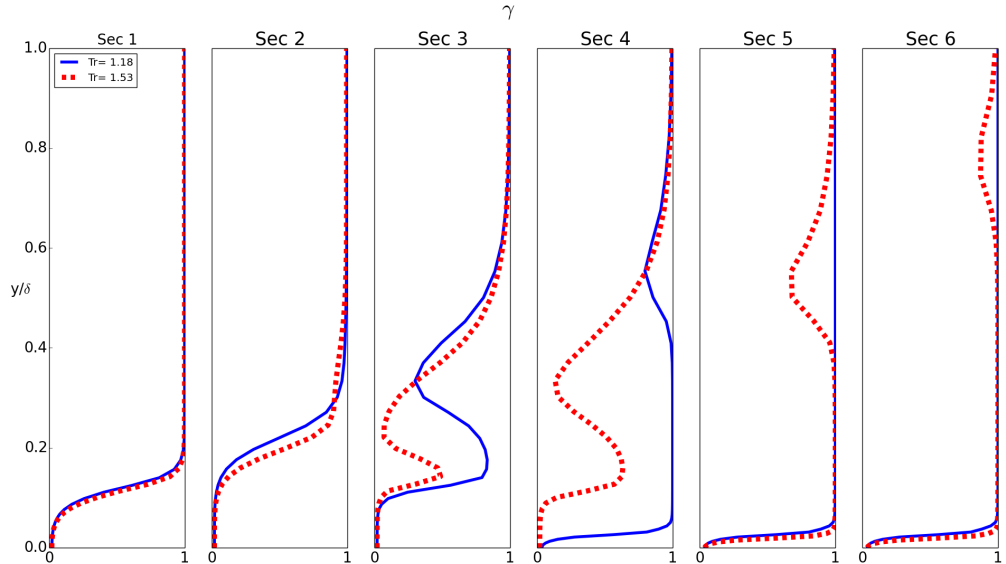


Figure 5.9: Intermittency

In Fig. 5.10 right is plotted the distribution of the Reynolds theta based on the momentum thickness. As explained in chapter three it is computed in the free stream according to empirical correlations then it is diffused inside the boundary layer. It is easy to see how for the case with higher temperature ratio, that means higher free stream temperature and pressure the value of this variable is always greater than for the case at lower temperature ratio. This could be a possible explanation for the higher temperature ratio the transition moves downstream.

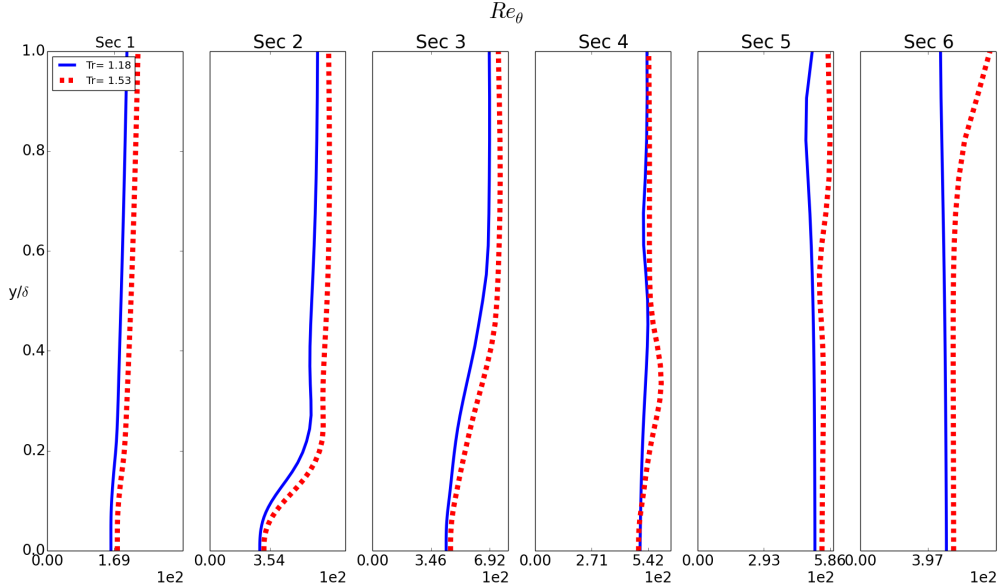


Figure 5.10: Momentum Thickness Reynolds Number

5.4 $\gamma - Re_\theta$ with $T_0 = 441[K]$

The first simulation campaign has been performed keeping the temperature of the blade constant and varying the free stream. However in the real machine the temperature of the free stream is approximately constant and the temperature ratio is reached lowering the temperature of the blade thanks to the cooling system. For this reason we choose to perform an other simulation campaign keeping the free stream value constant and reaching the same temperature ratio as before lowering the temperature of the wall. Author as Eckert and Kays [9, 13] in their works explains how the only parameters that has influence on the value of the HTC is the temperature ratio (ratio between the free stream temperature and the wall temperature). For this reason similar results are expected between the two cases taken into account.

Unfortunately we don't have experimental results with this boundary condition, however we expect a similar behavior in others to preserve the consistency of the model itself.

The boundary condition of the computations and the result are shown in the following table and in Tab. 5.4

$T_0[K]$	M_{2is}	Re_{2is}	Tu	$L_t[m]$	T_{ratio}
441	0.55	$9.5 \cdot 10^5$	0.8	0.02	1.18-1.38-1.53

Table 5.4: Boundary conditions for the $\gamma - Re_\theta$ at free stream conditions constant and low *FSTI*

The distribution of heat transfer coefficient shows that the model doesn't react in the

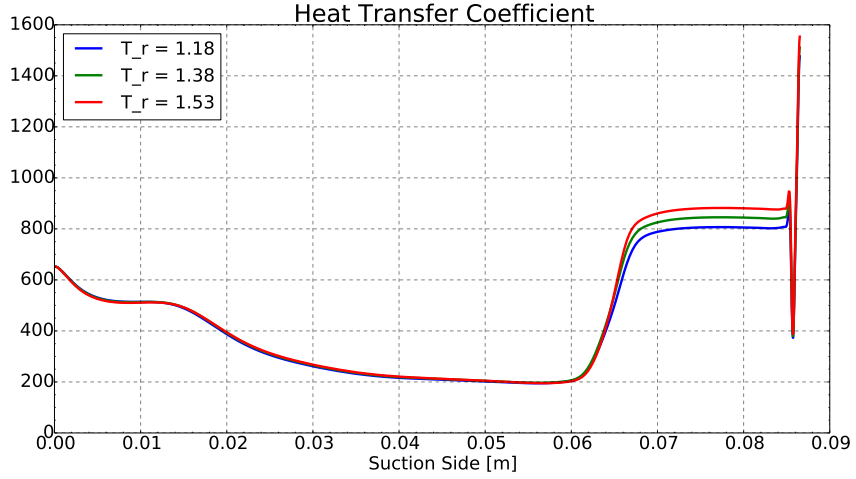


Figure 5.11: Heat transfer coefficient at constant Free Stream conditions

same way for the same temperature ratio changing the way to generate the temperature ratio. In fact if in the first simulation campaign the model shown a strong effect of the temperature ration on the transition in this case from the heat transfer coefficient distribution is not clear if the temperature ratio has some effect on the transition an if there is what is it.

Even if the results for the γRe_θ are not very encouraging we can still try to justify its behaviour. The analysis technique is the same presented in the previous section, we took six cut normal to the blade surface as draw in Fig 5.4 and we plot the principal field variables along them.

5.4.1 Kinematic quantities

As done for the previous case we analyze the velocity profiles inside the boundary layer. The conclusion we can drawn from the Fig 5.12 are similar to the one for the case with constant wall temperature. We can see how the velocity field is directly affected by the two different temperature ratio already in the laminar part in boundary layer. This is a further confirmation how in this kind of flow conditions the temperature field affects directly the velocity field also in case of same kinematic conditions.

5.4.2 Density and viscosity

The behaviour of the density ρ and dynamic viscosity μ are affected by the temperature field. The difference between this case and the one with T_{wall} constant is that in this case the free stream condition are the same so the variables are scaled respect to the the same value. From the Fig 5.14 it is clear how increasing the temperature ratio (cooling the surface of the blade) the density increases according to the perfect gas law while the viscosity decreases according to the Sutherland law.

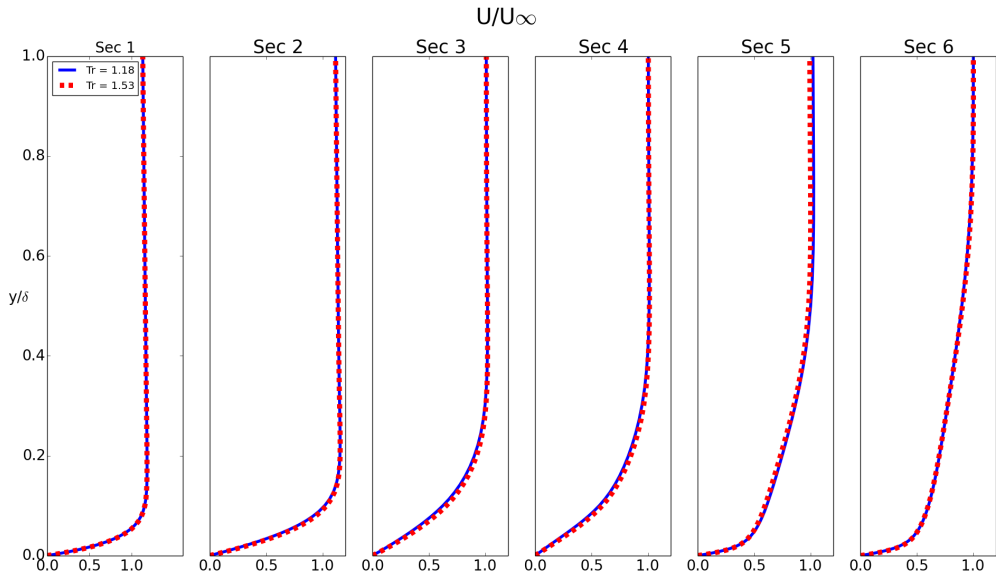


Figure 5.12: Velocity distribution inside the boundary layer at constant free stream conditions

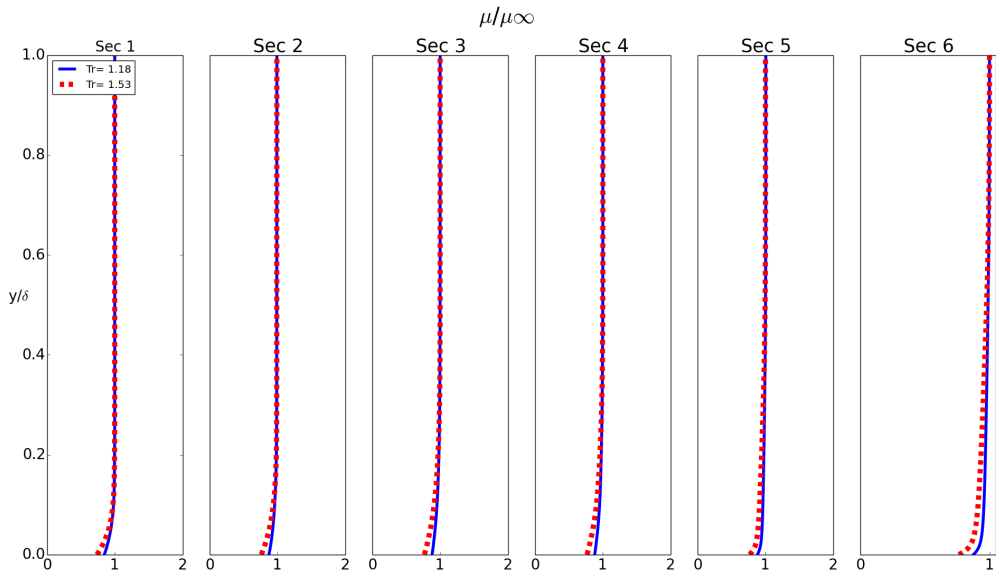


Figure 5.13: Dynamic Viscosity

In order to quantify the conjoint effect of the viscosity and the density could be useful to plot the kinematic viscosity $\nu = \frac{\mu}{\rho}$. It is clear how increasing the temperature ratio

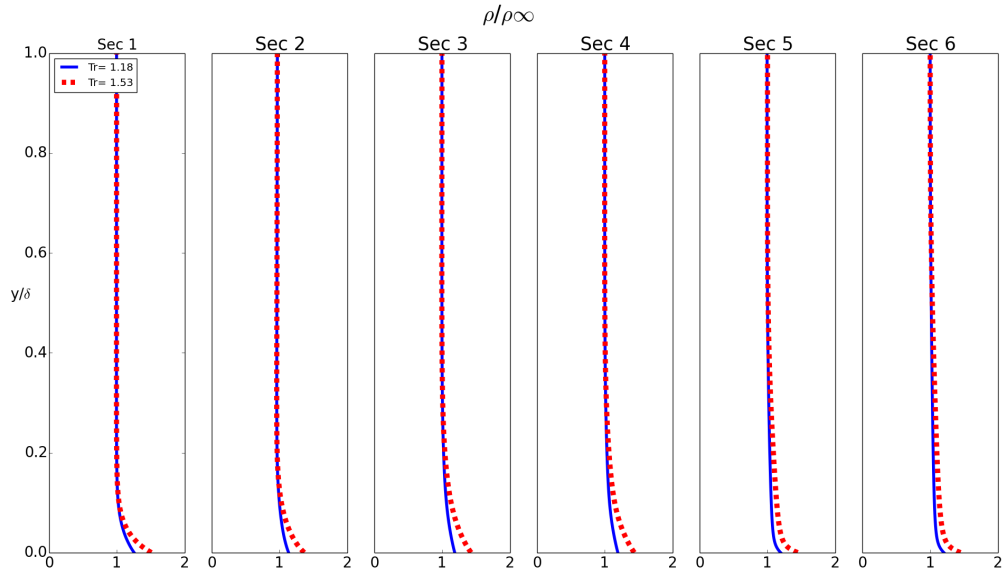


Figure 5.14: Density

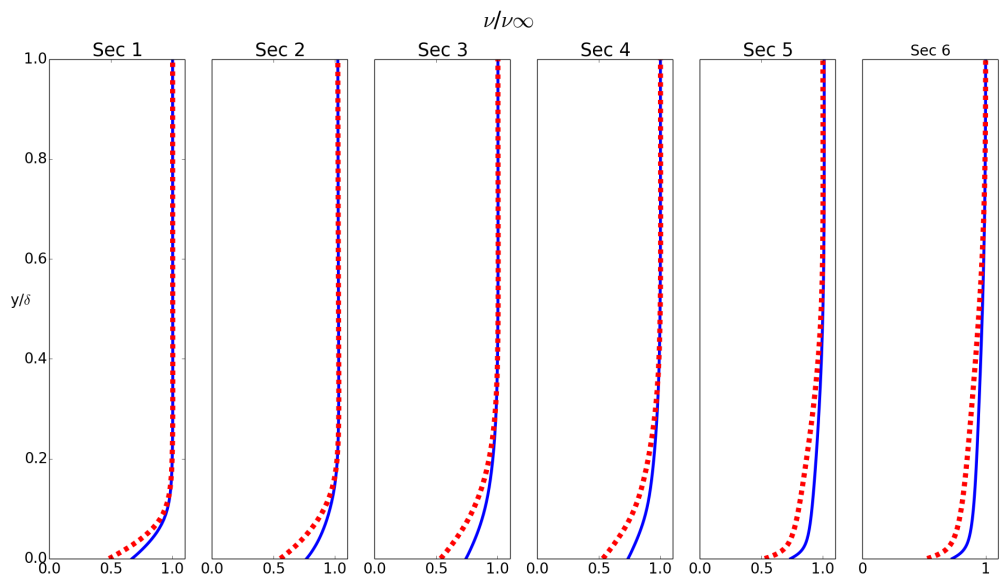


Figure 5.15: Kinematic Viscosity

the kinematic viscosity decreases, as expected from the behaviour of dynamic viscosity and density.

Finally it is interesting to notice how the influence of the temperature on the den-

sity and viscosity is propagated inside the boundary layer from the first section to the final one. This behaviour could have some interesting effects on the developing of the turbulent kinetic energy that we will see in the next section despite the transition took place in the same location has different evolution.

5.4.3 Turbulent quantities

The turbulent quantities we took into account are the intermittency function the momentum thickness Reynolds theta and the turbulent kinetic energy. About the intermittency function as expected, because the transition takes place at the same position, there are no differences both in the radial and stream wise evolution.

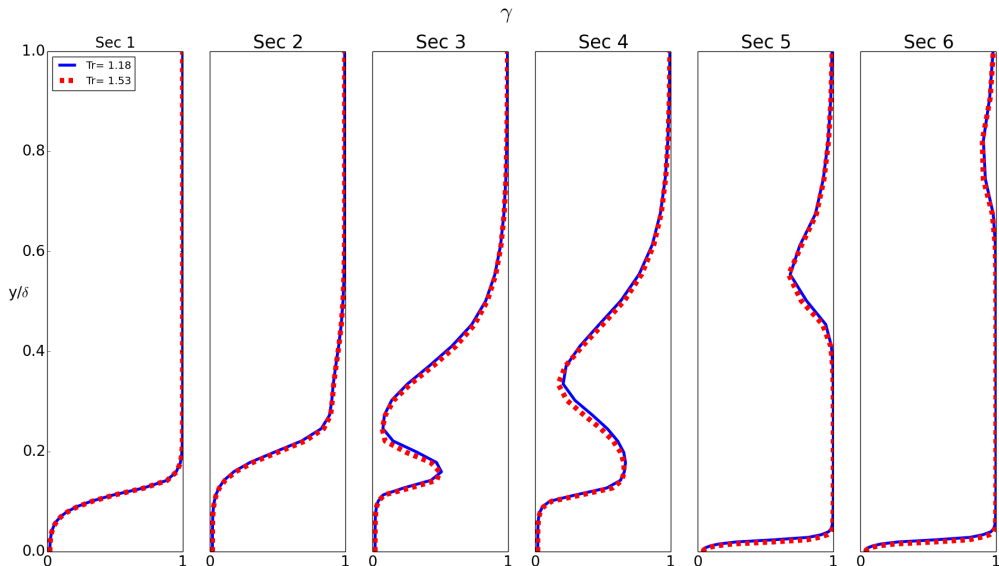


Figure 5.16: Intermittency

Also the distribution of the momentum thickness Reynolds number doesn't show differences between the two different temperature ratios. This is due to the fact that the equation from the momentum thickness Reynolds number is designed in order to diffuse in the boundary layer. Because the value of the free stream is compute with empirical correlation and is the same for the two different temperature ratios because the free stream conditions are identical also the diffusion in the boundary layer will leads to very similar values.

5.4.4 $\gamma - Re_\theta$ Conclusions

After this analysis we can conclude that the $\gamma - Re_\theta$ model is not able to reproduce the experimental results. In particular we found out that:

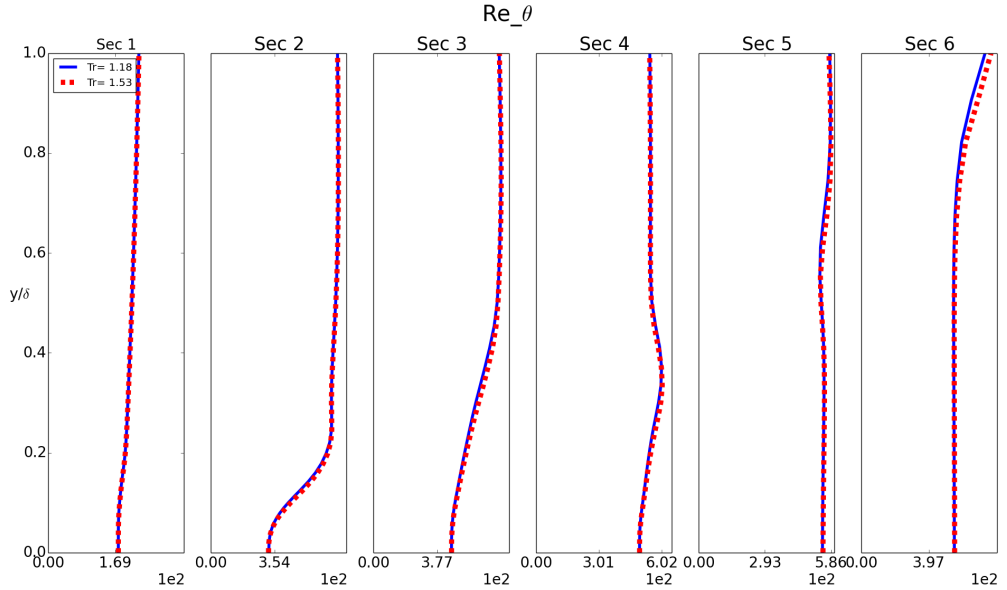


Figure 5.17: Momentum Thickness Reynolds Number

- For the case at constant wall temperature the model predict a stabilization of the flow increasing the temperature ratio while the experiments show the opposite.
- For the case at constant free stream conditions the model seems not be able to describe any dependency of the transition from the temperature ratio.

This behaviour can be explained analyzing the correlation that triggered the transition in the model. As explained in the Chapter 3 the transition is triggered once the following equation reach a certain value:

$$F_{onset} \sim \frac{R_v}{2.193 R_{\theta_c}} \quad (5.1)$$

The main parameters that drive the value of this expression are the kinematic viscosity ν contained in the vorticity Reynolds number and the value of the transition onset Reynolds results of the diffusion in the boundary layer of the value in the free stream coming from empirical correlations. The behaviour of the two different cases can be justify as follow:

- For the case at constant wall temperature the increase of the temperature ratio increase also the viscosity ratio between the free stream and the wall, this cause an increase in the value of the vorticity Reynolds number destabilizing the flow ???. However the variation of the onset momentum thickness Reynolds number due to the variation of the free stream is much higher respect to the one of the kinematic viscosity. The final results is that increasing the free stream temperature increases

a lot the value of Re_{θ_c} while causes a slightly variation of Re_v . As results the value of F_{onset} decrease increasing the free stream temperature. As results this cause a movement downstream of the transition location increasing the temperature ratio.

- For the case at constant free stream temperature the conclusions are similar. The temperature ratio cause a slightly variation of Re_v while the value of Re_{θ_c} remains the same. The mild variation of vorticity Reynolds number 5.19 is not able to influence the movement of the transition in an appreciable way.

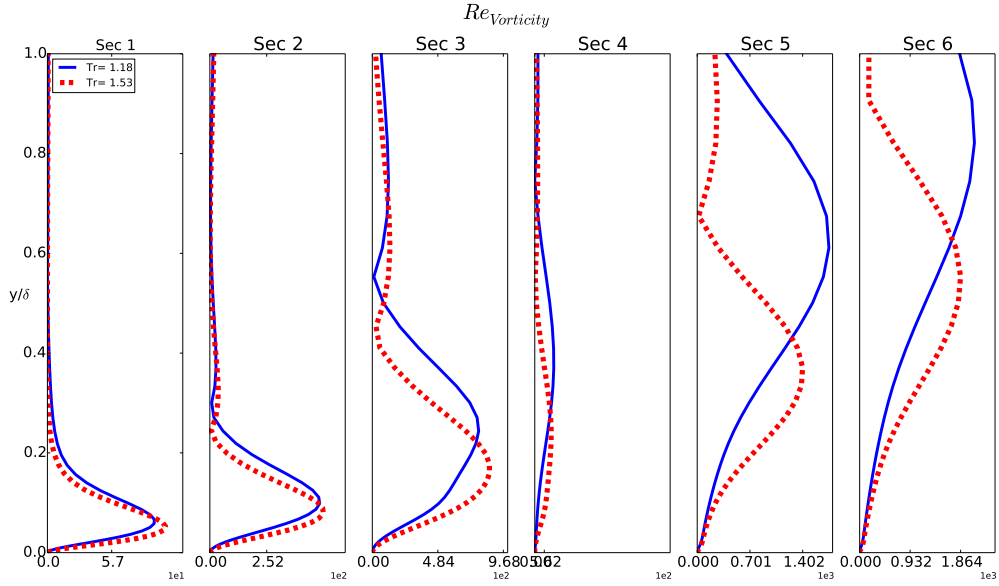


Figure 5.18: Vorticity Reynolds number for the case at constant wall temperature

Finally we can conclude that the behavior of the model is strictly correlated to the evolution of the momentum thickness Reynolds number in the free stream. The main limit probably is that the value of the momentum thickness Reynolds number is imposed in the free stream by empirical correlations calibrated on aerodynamic test cases. The behaviour of these correlations in case of thermal field is not still validated.

5.5 $k - k_l - \omega$

In this section the results obtained with the $k - k_l - \omega$ transition model are compared with the experimental ones. The boundary conditions are exactly the same as for the previous case and also in this case two different simulation campaigns have been performed: one keeping the wall temperature constant and varying the free stream conditions the other one keeping the free stream conditions constant and varying the wall temperature. The explanation of doing two different simulations campaign is the following: the case at

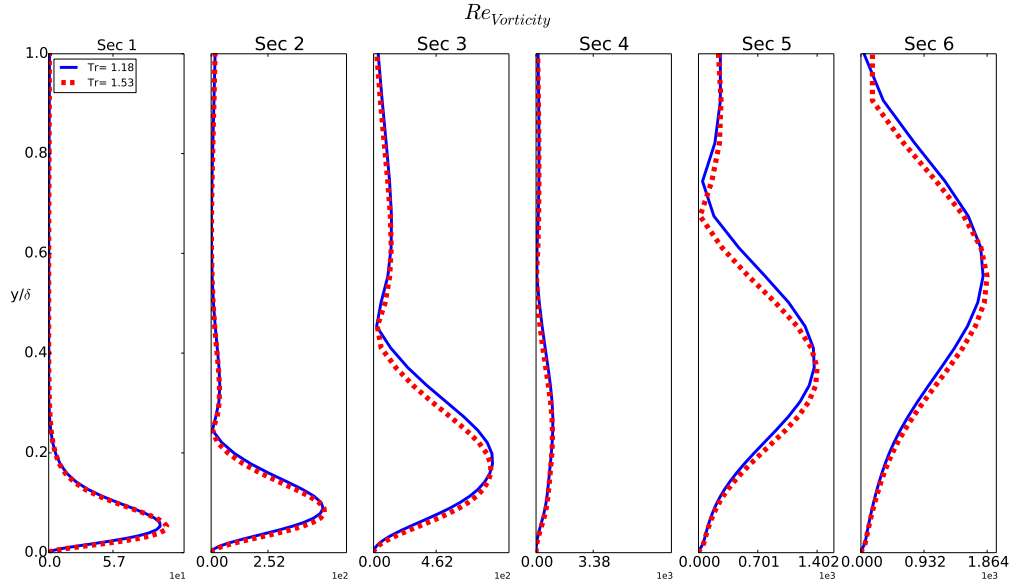


Figure 5.19: Vorticity Reynolds Number for the case at constant FS temperature

constant wall temperature is representative of the experiments and can be compared with the experimental result, while the other one is representative of the real machine working conditions, we expect that the model presents the same behaviour in the two different cases.

5.5.1 $k - k_l - \omega$ $T_{wall} = 294$

The first simulation campaign has been performed keeping constant the wall temperature and varying the free stream. The boundary conditions are the following:

$T_{wall}[K]$	M_{2is}	Re_{2is}	T_u	$L_t[m]$	T_{ratio}
294	0.55	$9.5 \cdot 10^5$	0.8	0.02	1.18-1.38-1.53

Table 5.5: Boundary conditions for the $k - k_l - \omega$ at wall temperature constant and low *FSTI*

The results coming from the computation have been compared with the experimental ones in order to understand if the trend predicted by the model is correct or not, the comparison is reported in Fig 5.23

It is interesting to notice how in this case the model is able to describe the right trend. In fact both the computations and the experiments show that an increase of the temperature ratio destabilizes the flow. The only evident difference is that according to the model the flow is continuously destabilized increasing the temperature ratio while according to the experiments seems that the sensitivity to the temperature ratio present

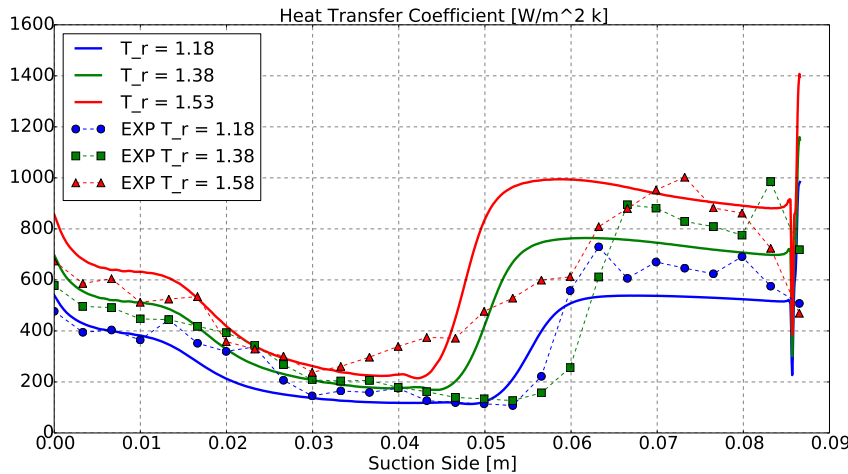


Figure 5.20: Heat Transfer coefficient

a certain threshold value.

In order to understand better what are the main variables of the model that drive this behaviour as done for the $\gamma - Re_\theta$ we have performed six cuts normal to the wall as sketched in Fig.5.4.

5.5.2 Velocity

The profiles of velocity show that: in the fully laminar and turbulent part of the boundary layer the velocity profile does not feel a strong influence of the different temperature field, the only difference is in the section 3, this is due the fact that the case with higher temperature ration has already reached transition while the blue one is still in a pre-transitional configuration. In fact, despite also in this case the thermal and kinematic field are coupled, the influence of the temperature on these variables seems weaker respect to the computation with the $\gamma - Re_\theta$.

5.5.3 Density and viscosity

As explained previously for the simulation campaign with the $\gamma - Re_\theta$ the effect of the temperature on density and viscosity is opposite. The temperature ratio increases the variation of density between the free steam and the wall while decrease the variation of dynamic viscosity. In both models in order to take into consideration the conjoint effect of both quantities is the kinematic viscosity. From Fig 5.24 the overall effect is a decrease of the kinematic viscosity.

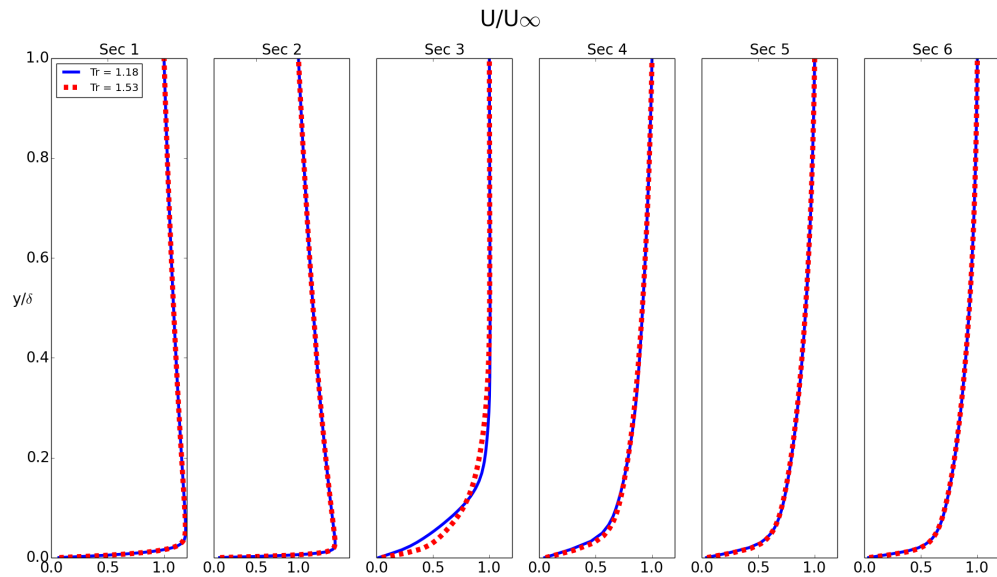


Figure 5.21: Absolute Velocity

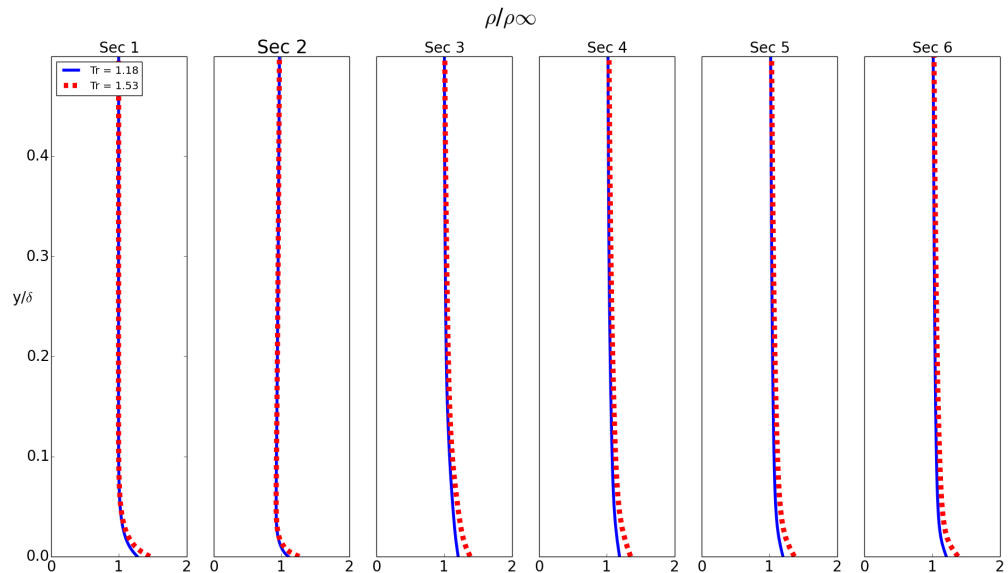


Figure 5.22: Density

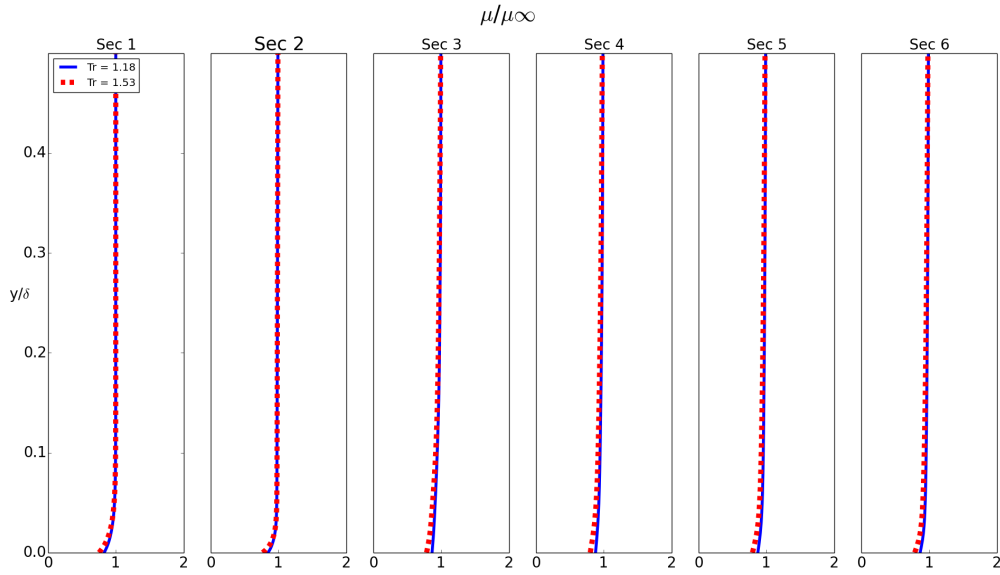


Figure 5.23: Dynamic Viscosity

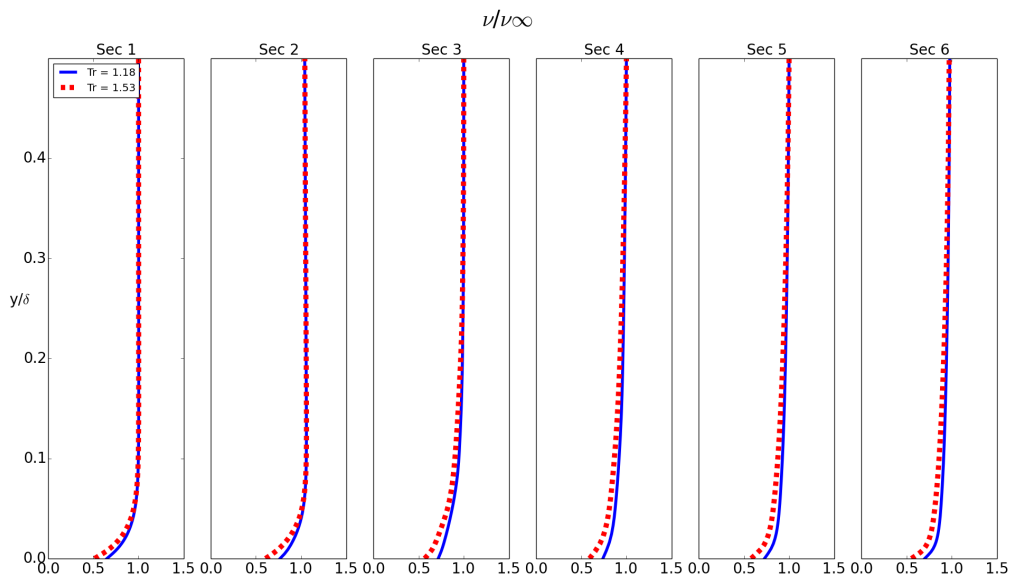


Figure 5.24: Kinematic viscosity

5.5.4 Turbulent variables

As explained in the Chapter 3 the philosophy of the model is to describe the transition process as an energy transfer between the large scale (laminar fluctuations) and the

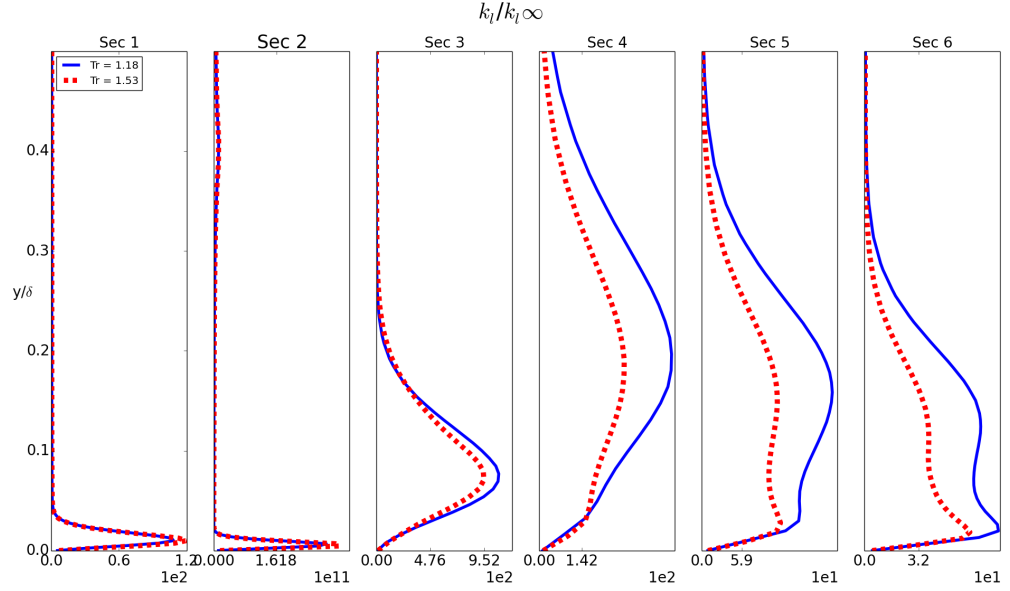


Figure 5.25: Laminar Kinetic Energy

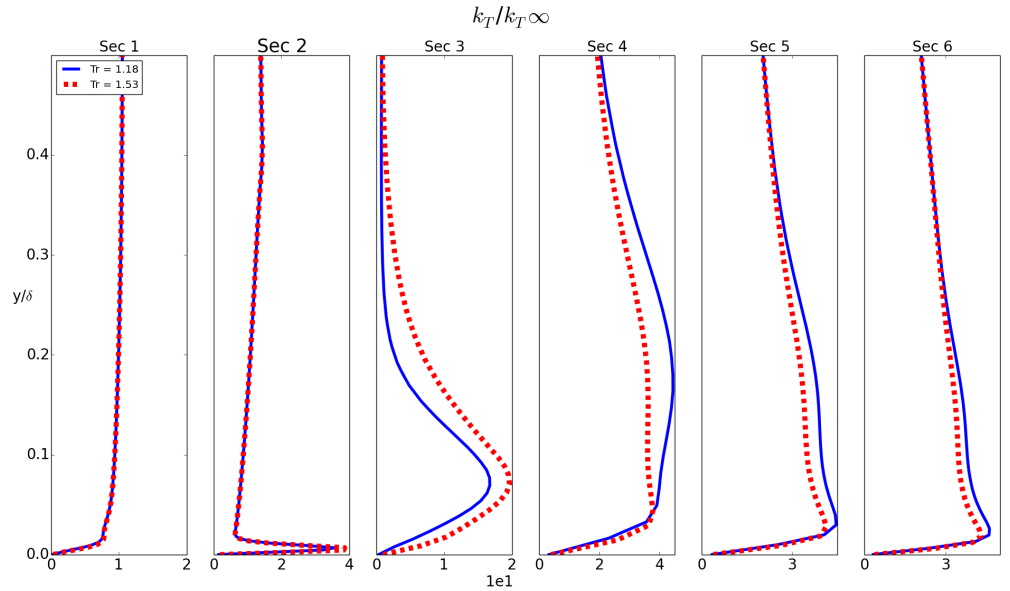


Figure 5.26: Turbulent Kinetic Energy

smaller scale (turbulent fluctuations). In Fig 5.25 are reported the distribution of laminar kinetic energy and turbulent kinetic energy 5.26 . From the laminar kinetic energy is easy to see that for the case at higher temperature ratio where the transition is more

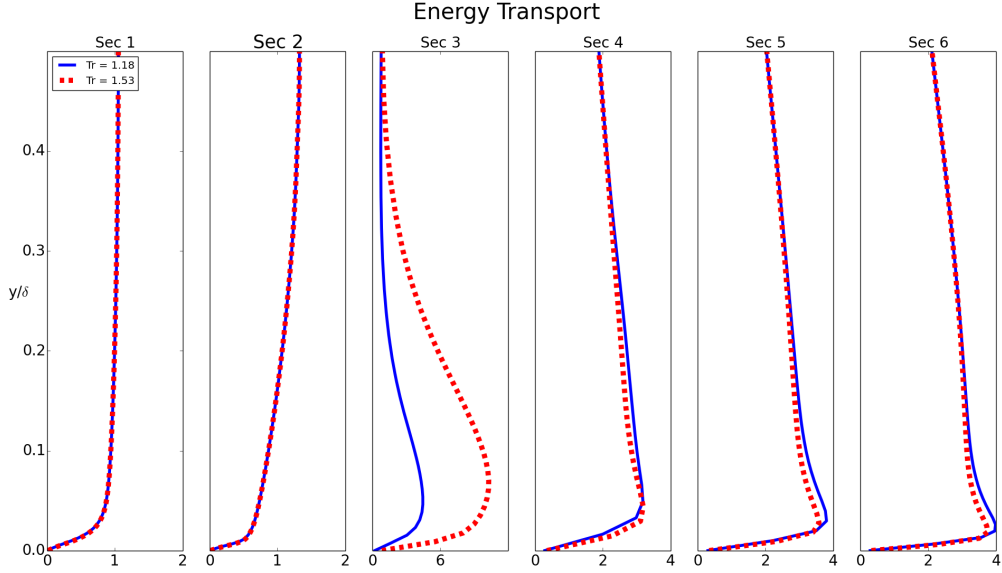


Figure 5.27: Energy Transfer

upstream there is a big enhancement of the laminar kinetic energy in section 3 while for the case at lower temperature ratio the enhancement is more pronounced in section 4. The same behaviour can be observed for the turbulent kinetic energy: we can observe an increase of its value where the transition is triggered. Finally in Fig 5.27 we can observe the behaviour the ratio of transport of energy from the large scales to the smaller scales described by the term: $R_{BP} = \beta_{BP} k_L \frac{\omega}{f_w}$

We can observe from the graph how in the section 3 near the transition location there is a big enhancement of the transport between the laminar and turbulent part of the total fluctuation energy.

5.5.5 $k - k_l - \omega$ $T_0 = 441$

This simulation campaign has been performed in order to check the consistency of the model. The boundary conditions for the simulations are the following:

$T_0[K]$	M_{2is}	Re_{2is}	Tu	$L_t[m]$	T_{ratio}
441	0.55	$9.5 \cdot 10^5$	0.8	0.02	1.18-1.38-1.53

Table 5.6: Boundary conditions for the $k - k_l - \omega$ at free stream conditions constant and low $FSTI$

The interesting fact is that in this case the model show the same trend as for the case with constant wall temperature. This could be due to the fact that ,respect to the

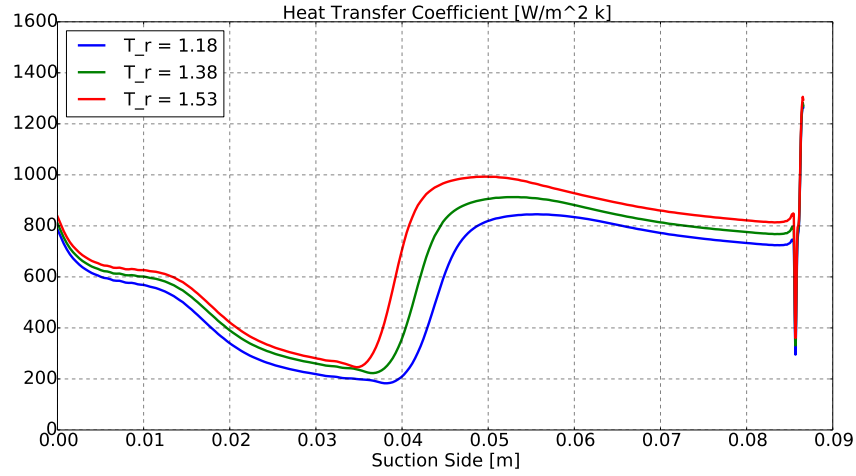


Figure 5.28: Heat Transfer coefficient

$\gamma - Re_\theta$, this model relies less on empirical correlation and try to describe more the physic involved in the process.

5.5.6 Velocity

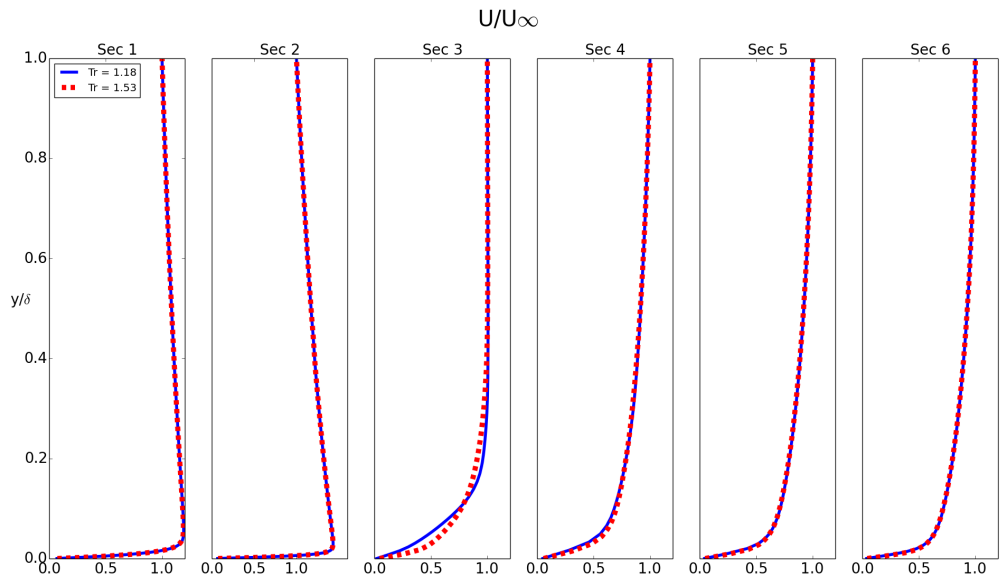


Figure 5.29: Absolute Velocity

Because the behaviour of the transition the same for the two cases the evolution of

the velocity profiles along the blade is similar to the simulation performed at constant blade temperature. In Fig 5.29 are reported the velocity profiles along the suction side.

5.5.7 Density and viscosity

Because of the the graph are plotted in non dimensional variables respect to the value of the free stream values the relative variation of quantities like density and viscosity is the same for two cases taken into consideration. In particular as explained in the section 5.3.2 the density increases at the wall due to the temperature ratio while the viscosity decreases. In order to be able to capture the the conjoint of the variation of both density and dynamic viscosity we choose to plot the value of the kinematic viscosity in Fig 5.30. We can observe how the behaviour is qualitatively the same respect to the other simulations performed both with the $\gamma - Re_\theta$ and the $k - k_l - \omega$, the only difference is that seems that the penetration of the thermal effects inside the boundary layer seems to be weaker for the cases with the $k - k_l - \omega$ respect the one with the $\gamma - Re_\theta$.

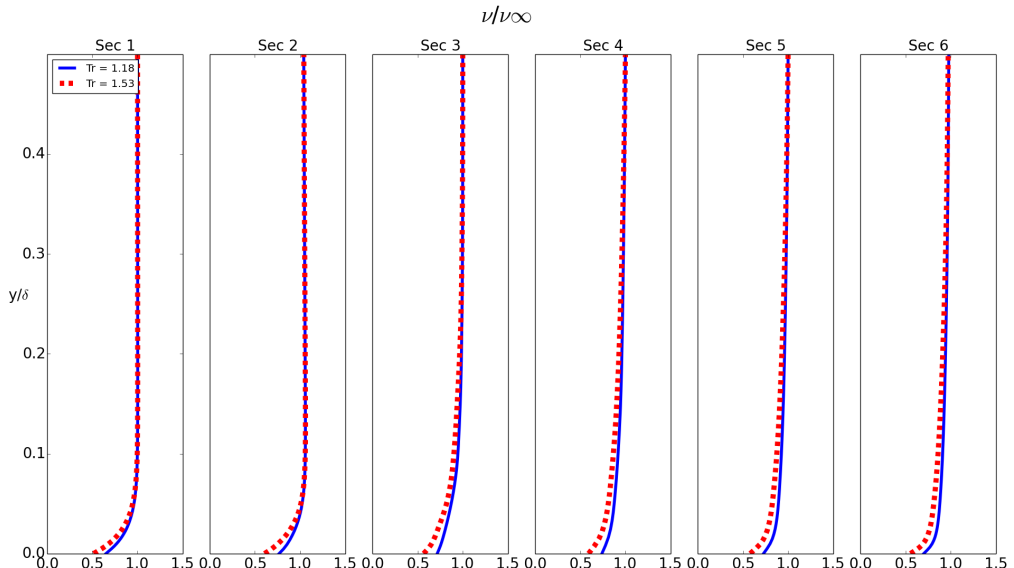


Figure 5.30: Kinematic viscosity

5.5.8 Turbulent variables

Finally as we did for the previous case we report the behaviour of the turbulent and laminar kinetic energy and the distribution of the energy transfer between the two scales. In this case is more difficult to draw any conclusions because the transition move less than in the simulation with constant wall temperature. However the interesting features in order to try to understand the behaviour of the model are the following:

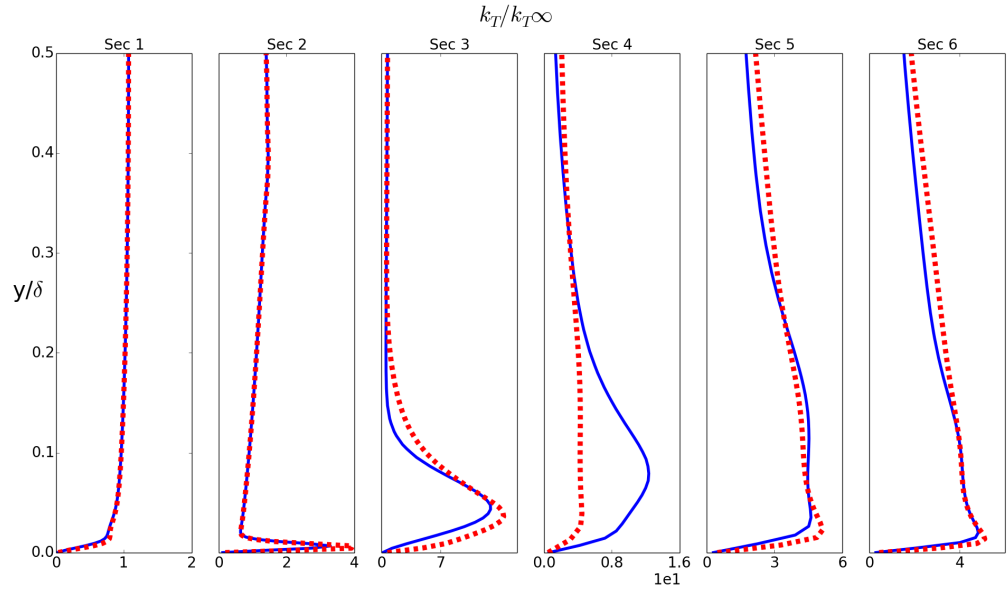


Figure 5.31: Turbulent Kinetic Energy

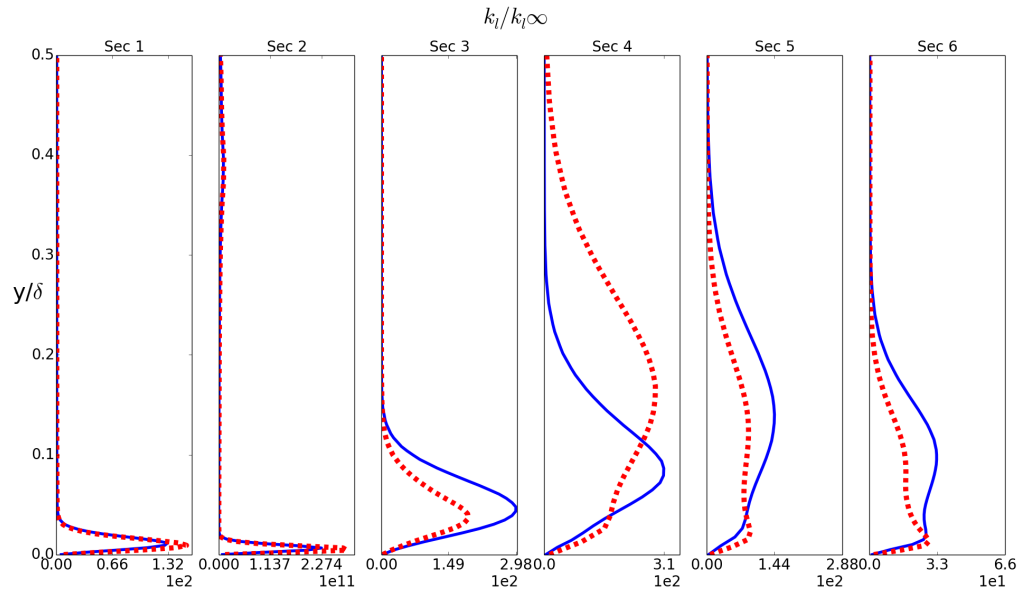


Figure 5.32: Laminar Kinetic Energy

- The distribution of the laminar kinetic energy 5.32 shows how for the higher temperature ratio the maximum is located in the section 3 while for the lower temperature ratio in the section 4. This could be due to the fact that for the higher

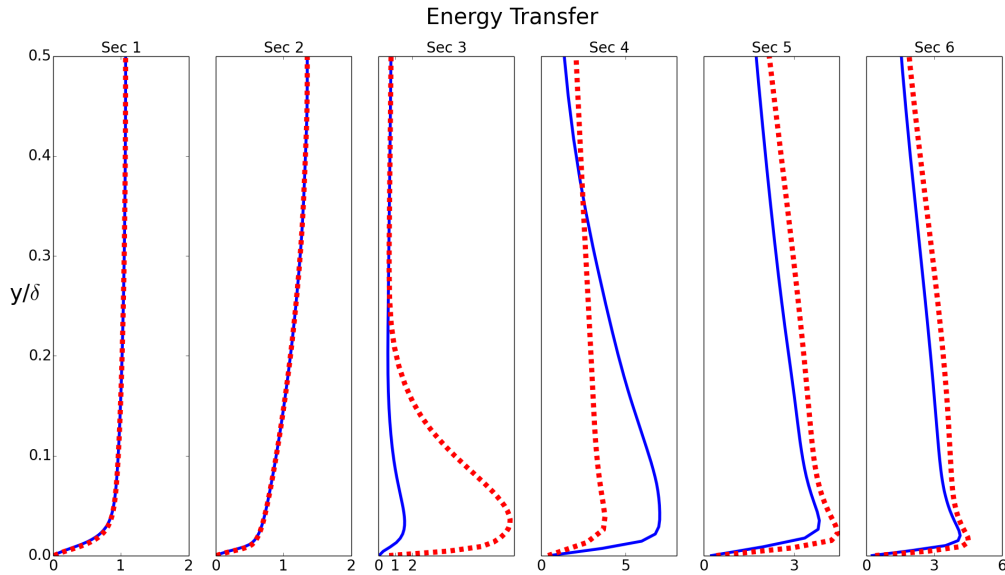


Figure 5.33: Energy Transfer

temperature ratio the transition starts earlier and so does the transport of energy from the large scale to the smaller scale

- The behaviour of the turbulent kinetic energy 5.31 can be explained by the distribution of the energy transfer. From the plots it is easy to see how for the higher temperature ratio the transfer start earlier (in section 3) than for the lower temperature ratio (section 4). This is a possible consequences of the movement of the transition.

As for the case at constant wall temperature the maximum of the energy transfer is located in the section 3 for the higher temperature ratio and in the section 4 for the lower temperature ratio. This behaviour could be correlated to the movement of the transition: upstream for the case with higher temperature ratio and downstream for the case with lower temperature ratio.

5.5.9 $k - k_l - \omega$ Conclusions

The behaviour of the $k - k_l - \omega$ model is very encouraging. In the three tests cases with blade temperature constant tested in the wind tunnel the comparison between the experimental results and the computation shows that although the model is not able to predict very accurately the absolute value of heat transfer and the transition location, it is able to reproduce the right behaviour of the transition as the temperature ratio increases. Moreover the behaviour of the model doesn't change if we apply the same temperature ratio but keeping the free stream constant.

This behaviour could be due to the fact that the model relies less of empirical correlations and more on physical considerations. As explained in the chapter 3 the philosophy of the model is to track the evolution of the pre-transitional fluctuations (laminar kinetic energy), when they reach a certain value they activate a threshold function that trigger the transport of energy from the larger scale to the smaller ones. The threshold function is :

$$\phi_{BP} = \max\left[\frac{k_T}{\nu\Omega} - C_{BPcrit}, 0\right] \quad (5.2)$$

We can see how the main variables that drives the value of ϕ_{BP} are the turbulent kinetic energy k_T the vorticity Ω and the kinematic viscosity ν . From the cuts presented before we can observe how at least in the pre-transitional part of the boundary layer the turbulent kinetic energy and the vorticity are very similar, due to the same shape of the velocity profile, for the two temperature ratios. However the kinematic viscosity related to the free stream value shows a bigger decrease for the case at higher temperature ratio. It is reasonable to believe that the variation of the viscosity inside the boundary layer is the main cause of the variation of the threshold function leading to a destabilization of the flow.

The reasons of the good behaviour of this kind of model respect to the previous one could be attributed to the fact that the relations used to trigger the transition are based on physical parameters of the flow like viscosity and density instead of rely on empirical correlations. A reason of the consistency of the model in both test cases analyzed could lay in the fact that the behaviour of the thermo physical quantities according to the variation of temperature is easier to describe while tuning a correlation for such a different and demanding conditions is certainly much more tricky.

5.6 Experimental results with high free stream turbulence intensity

For sake of completeness we report an extra experimental and computational campaign performed at the same exit Reynolds number but with an higher Mach number and higher turbulence intensity. The boundary conditions for the computation are the following:

$T_{wall}[K]$	M_{2is}	Re_{2is}	Tu	$L_t[m]$	T_{ratio}
294	0.83	$9.5 \cdot 10^5$	5.3	0.02	1.18-1.38-1.53

Table 5.7: Boundary conditions for the case at high turbulence intensity

The Fig 5.34 (left) reports the value of the heat transfer coefficient on the blade surface measured during the experiments while in Fig 5.34 (right) the results from the computations.

Unfortunately with this boundary conditions we are not able to see any effect of the temperature on transition neither from experimental results nor from numerical

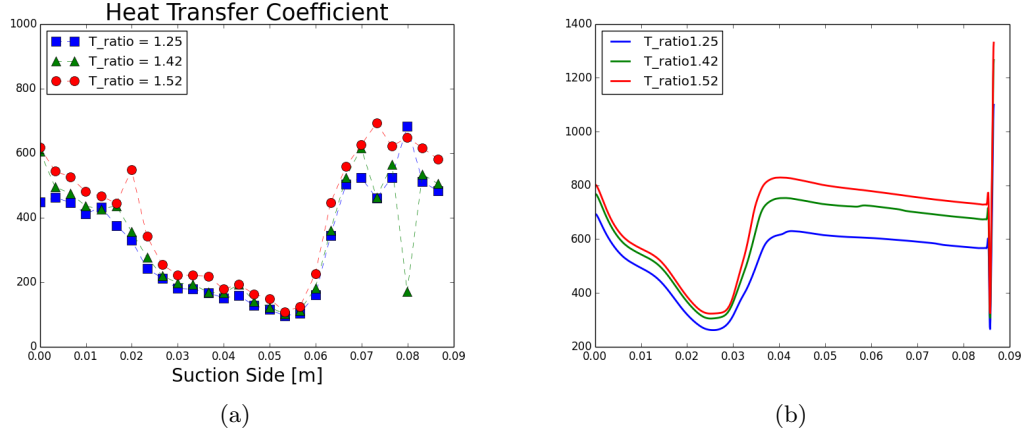


Figure 5.34: Heat Transfer Coefficient from the experiment left and computation right

computations. This could be due to the fact explained in the beginning of this chapter: the temperature has a marginal effect respect to the turbulence intensity and pressure gradient. So the too high value of turbulence intensity completely overcomes any possible effects of the temperature. From the value of the heat transfer coefficient measured from the experiments is not clear evidence of a possible influence of the temperature on the transition location, the only effects that seem present are a modification of the transition length and of the absolute value of the heat transfer coefficient in the fully turbulent part. From the numerical point of view the conclusion about these test case are similar: there are no clear effects on the effect of the temperature ratio on the movement of the transition location, the only effects that seem to be present are on the developing of the transition itself and on the absolute value of the heat transfer coefficient in the fully turbulent part of the boundary layer.

Chapter 6

Conclusions and future works

6.1 Conclusions

The main target of this work was to understand the capabilities of the stat of art transition models to describe the effect of the gas to wall temperature ratio on the transition. The transition models chosen for this analysis are the $\gamma - Re_\theta$ [19] and the $k - k_l - \omega$ [28]. In order to understand the real capabilities of the transition models the results coming from the computation has been compared with the experimental results provided by an other parallel research master project. From the experimental point of view the strategy chosen to reach the right temperature ratio is to keep the temperature of the blade constant and to vary the temperature of the free stream keeping the same Mach and Reynolds number. For each transitional model two simulation campaigns have been performed:

- The first with the same conditions as the experiments.
- The second with the same temperature ratio, Mach and Reynolds of the experiments but keeping the free stream constant and chancing the wall temperature.

The reason of performing two tests is that the first case is more representative of the experimental condition and is needed to compare the results, the second one is more representative of the working conditions of the real machine. We expect that the results show the same trend in order to the model be consistent with itself.

After the simulations we obtain the following results:

6.1.1 $\gamma - Re_\theta$

The $\gamma - Re_\theta$ is not able to predict the right behaviour whit the variation of the temperature ratio. In fact we observe that:

- For the case of constant wall temperature the experiments show how increasing the gas to wall temperature ratio causes the movement of the transition location

upstream. The model predicts the opposite trend, this is due to the evolution of the free stream value of the momentum thickness Reynolds number inside the boundary layer as explained in the previous chapter.

- For the case at constant free stream temperature is not evident any movement of the transition location. The explanation could be found in the fact that same free stream values lead to the same value of Re_θ diffused inside the boundary layer, this fact overcomes the effect of the temperature.

The conclusion is that the $\gamma - Re_\theta$ is not able to predict the same results as the experiments for this kind of operations conditions. Moreover we have shown that the model is not consistent with itself when we change the way of applying the temperature ratio.

6.1.2 $k - k_l - \omega$

Exactly the same procedure has been applied for the simulation campaign with the $k - k_l - \omega$ mode. In this case the results are more encouraging: in fact the model is able to predict the same behaviour of the experimental results in the case of constant wall temperature. The only differences is that the experimental results show a threshold value after which the movement of the transition point is triggered while the model shows a continuous destabilization increasing the temperature ratio.

The interesting fact is that, as opposite of the $\gamma - Re_\theta$, the model shows the same behaviour also in the simulations with constant free stream conditions, this is probably due to the stronger dependency of the transition criterion on value of viscosity near the wall.

6.2 Future works

The results of the following works show how the two state of art RANS transitional models analyzed ($\gamma - Re_\theta$ and $k - k_l - \omega$). The results are pretty encouraging in particular for the $k - k_l - \omega$ in fact it showed to have the same behaviour of the experimental results and moreover to be dependent only from the value of the temperature ratio and not from this ratio is reached. However a lot remains to do, in particular the next steps in order to go deeper into the topics are:

- A better understanding of the equivalence between the real working conditions of the machine (constant free stream and T_{wall} variable) and the the experimental conditions (constant T_{wall} and free stream variables). This point is important because according to the literature at the same working conditions only the T_{ratio} should matter in determining the value of the HTC, however both model shown a different behaviour.
- Deeper analysis of the internal working of the model. In this project work the models have been used "as they are" whit the value of the free parameters calibrated

on benchmark test cases quite far from the conditions used in this analysis. It could be of great interest try to understand if it is possible to generalize the models thanks to a more general calibration of the free parameters on experimental results more close to the real working condition of the machine.

- So far we focus our effort on the study of the behaviour of the model in describe a certain physics hopefully catch from the experimental results. However different temperature ratios affect the physic of the bypass transition is a very cutting edge topic by itself. One of the most challenging development of the project could be try to perform high order simulation (LES) in order to see if it is possible to understand more about the physics underlying the phenomenon. The possibility of a large eddy simulation has been proposed in the beginning part of the project however it has been abandoned due to the lack of time in order to focusing on the results coming from the RANS computations. The major difficulties of a large eddy simulation encountered are: the first one the extremely large number of cells needed in order to resolve till the Taylor length scale for a flow at Reynolds number around 10^6 , another challenging aspect is the the way to impose the inlet free stream turbulent intensity, a possible way has been found in one of the last release of OpenFoam [1] 1612+ in whit a boundary condition for LES that impose the right turbulence intensity has been implemented, however because of the lack of time this part of the project has not been deepened completely.

Appendix A

Boundary Conditions

In the first part of this appendix we will show how the boundary conditions from the experiment has been converted in order to be used in a CFD simulation. In the second part we will explain the procedure in order to compute the right value of the turbulent variables ($FSTI$ and L_t) for the simulations with the $k - k_l - \omega$ model.

A.1 Boundary Condition Conversion

In the experimental campaign it is easy to measure the values of:

- Inlet Total Temperature
- Exit isoentropic Mach number
- Exit isoentropic Reynolds number

However in order to perform a CFD computation, for theoretical reasons, we need to have two information at in inlet boundary and one information at the outlet boundary. The needed quantities are:

- INLET :
 - Total Pressure
 - Total Temperature
- OUTLET : Static pressure

Fortunately it is possible to compute in a univocal way the needed quantities (P_T, T_T and P_s) from the known quantities ($T_T, Mach_2, Re_2$).

The procedure is the following:

From the value of total pressure and Mach number is possible to retrieve the value of the static pressure:

$$T_{2is} = \frac{T_{T0}}{1 + \frac{\gamma-1}{2} * M_{2is}^2} \quad (\text{A.1})$$

And the value of the absolute velocity from the value of the Mach number:

$$U_{2is} = \sqrt{\gamma R T_{2is}} \quad (\text{A.2})$$

From the temperature the value of the viscosity thanks to the Sutherland law:

$$\mu_{2is} = 1.458 \cdot 10^{-6} \frac{T_{2is}^{1.5}}{110,4 + T} \quad (\text{A.3})$$

Knowing the value of the Reynolds number we can compute the value of the density:

$$\rho_{2is} = \frac{Re_{2is} \mu_{2is}}{U_{2is} chord} \quad (\text{A.4})$$

The value of the static pressure from the perfect gas law:

$$P_{2is} = \rho_{2is} R T_{2is} \quad (\text{A.5})$$

Finally we can compute the value of the total pressure from:

$$P_0 = P_{2is} \left(\frac{T_{T0}}{T_{2is}} \right)^{\frac{\gamma}{\gamma-1}} \quad (\text{A.6})$$

The procedure has been implemented in the following C++ script:

```
#include <iostream>
#include <math.h>
using namespace std;

int main()
{
    double T0;
    double M2is;
    double Re2is;
    double T2is;
    double U2is;
    double mu2is;
    double rho2is;
    double p2is;
    double P01;

    double Gamma=1.4;
    double R=287;
    double mu0=1.716e-5;
```

```

double C=110.4;
double Tref=273.15;
double chord=63e-3;

cout<<"Inlet Total Temperature : ";
cin>> T0;

cout<<"Outlet Isoentropic Mach Number : ";
cin>>M2is;

cout<<"Outlet Isoentropic Reynolds Number : ";
cin>>Re2is;

T2is=T0/(1+0.5*(Gamma-1)*M2is*M2is) ;
U2is=M2is*sqrt(Gamma*R*T2is);
mu2is=mu0*pow((T2is/Tref),1.5)*(Tref+C)/(T2is+C);
rho2is=Re2is*mu2is/U2is/chord;
p2is=rho2is*R*T2is;
P01=p2is*pow((T0/T2is),Gamma/(Gamma-1));

cout<<"Total Pressure Inlet : "<<P01<< endl ;
cout<<"Total Temperature Inlet : "<<T0 << endl;
cout<<"Static Pressure Outlet : "<< p2is << endl;

return 0;
}

```

A.2 Turbulent boundary conditions

The turbulence transition models are very sensitive to the inlet boundary conditions on the variables of the transition model itself, such as free stream turbulence intensity and turbulent integral length scale. In particular with the simulations with the $k - k_l - \omega$ we noticed that the turbulence decades in the part of the domain between the inlet and the leading edge stronger than expected. So in order to obtain results coherent with the experimental ones we have to impose a value in the inlet such as the measured value at the leading edge will be the same at the one measured from the experiments. This has been done computing the evolution of the turbulent kinetic energy k_T and the specific dissipation rate ω according with the approximated expressions:

$$U_\infty \frac{dk_T}{ds} = -\omega k_T \quad (\text{A.7})$$

$$U_\infty \frac{d\omega}{ds} = -C_{\omega 2}\omega^2 \quad (\text{A.8})$$

The evolution has been computed with an Euler explicit method in the following python script:

```

import numpy as np
import matplotlib.pyplot as pl

def ODE_system(k,omega):
    U_inf = 60
    C = 1.92

    k_dot = -omega*k/U_inf # put minus to go downward or plus backward
    omega_dot = -C*omega*omega/U_inf

    return k_dot,omega_dot

dx = 0.0001
x_ini = 0
x_fin = 0.059

nstep = int(np.ceil((x_fin-x_ini)/dx))
x = np.linspace(x_ini,x_fin,nstep+1)

#initialize array
k_s = np.empty((nstep +1,))
omega_s = np.empty((nstep+1,))

#initial value
k_s[0] = 0.54
omega_s[0] = 73 # 0.09**0.75*(k_s[0]**1.5)/0.01

#solve the system
for k in range(nstep):
    k_dot,omega_dot = ODE_system(k_s[k],omega_s[k])

    k_s[k+1] = k_s[k] + k_dot*dx
    omega_s[k+1] = omega_s[k] + omega_dot*dx

```

```
epsilon = 0.09*omega_s*k_s

#plotting

f1 = pl.figure(1)
pl.rcParams[ 'axes.facecolor' ] = 'white'
f1.patch.set_facecolor('white')

pl.plot(x,k_s)
pl.plot(x[0],k_s[0],'ro')
pl.plot(x[nstep],k_s[nstep],'ro')
pl.xlabel('x')
pl.ylabel('k')
pl.title('K')
pl.grid(b=True, which='major', color='r', linestyle='--')

f2 = pl.figure(2)
pl.rcParams[ 'axes.facecolor' ] = 'white'
f2.patch.set_facecolor('white')

pl.plot(x,omega_s)
pl.plot(x[0],omega_s[0],'ro')
pl.plot(x[nstep],omega_s[nstep],'ro')
pl.xlabel('x')
pl.ylabel('$\omega$')
pl.title('$\omega$')
pl.grid(b=True, which='major', color='r', linestyle='--')

f3 = pl.figure(3)
pl.rcParams[ 'axes.facecolor' ] = 'white'
f3.patch.set_facecolor('white')

pl.plot(x,epsilon)
pl.plot(x[0],epsilon[0],'ro')
pl.plot(x[nstep],epsilon[nstep],'ro')
pl.xlabel('x')
pl.ylabel('$\epsilon$')
pl.title('$\epsilon$')
pl.grid(b=True, which='major', color='r', linestyle='--')

print(' x_fin = ' + str(x[nstep]) + ' k_s = ' + str(k_s[0]) + '\ \ omega_s = ' +
print(' x_0 = ' + str(x[0]) + ' k_s = ' + str(k_s[nstep]) + '\ \ omega_s = ' + st
```

```
pl.show()
```

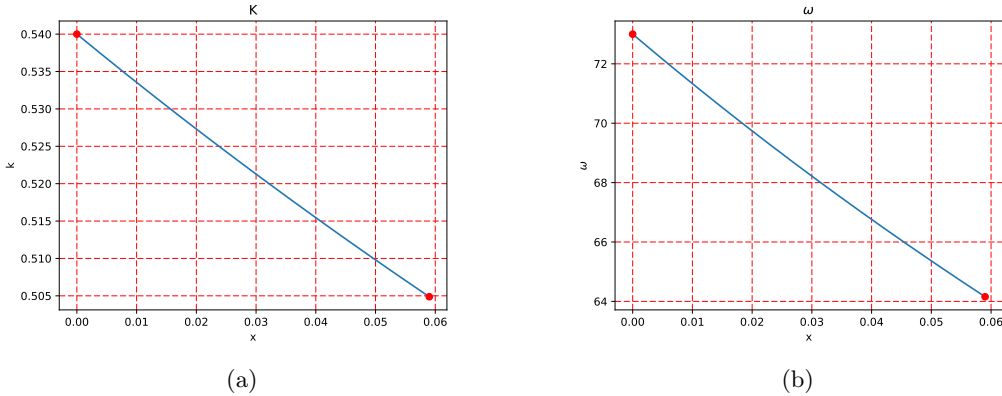
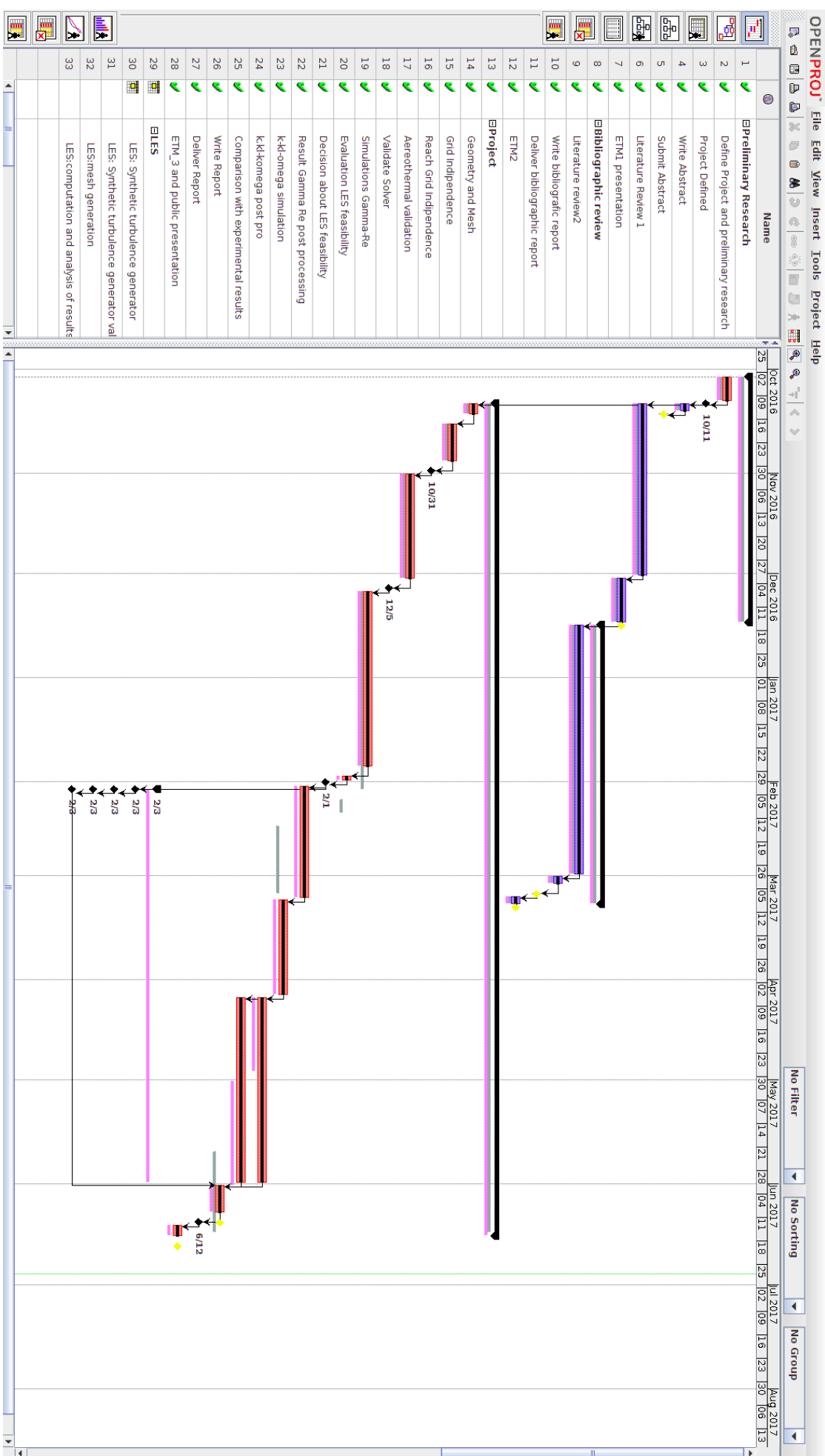


Figure A.1: Decay of a) turbulent kinetic energy b) specific dissipation from the inlet section from the LE

Appendix B

Planning



References

- [1] Openfoam. [http://www.openfoam.com/version-v1612+/.](http://www.openfoam.com/version-v1612+/)
- [2] *User Manual Fine Turbo 9.1.*
- [3] BJ Abu-Ghannam and R Shaw. Natural transition of boundary layersthe effects of turbulence, pressure gradient, and flow history. *Journal of Mechanical Engineering Science*, 22(5):213–228, 1980.
- [4] Daniel Arnal and Olivier Vermeersch. Compressibility effects on laminar-turbulent boundary layer transition. *International Journal of Engineering Systems Modelling and Simulation*, 3(1-2):26–35, 2011.
- [5] T. Arts and L. De Rouvroit. *Aero-thermal investigation of a highly loaded transonic linear turbine guide vane cascade - A test case for inviscid and viscous flow computations.* von Karman Institute for Fluid Dynamics, Rhode-St-Genese, Belgium, 1990.
- [6] Kuei-Yuan Chien. Predictions of channel and boundary-layer flows with a low-reynolds-number turbulence model. *AIAA journal*, 20(1):33–38, 1982.
- [7] Marco Costantini, Uwe Fey, Ulrich Henne, and Christian Klein. Nonadiabatic surface effects on transition measurements using temperature-sensitive paints. *AIAA Journal*, 53(5):1172–1187, 2015.
- [8] L. Cutrone, P. De Palma, G. Pascazio, and M. Napolitano. An evaluation of bypass transition models for turbomachinery flows. *International journal of heat and fluid flow*, 28(1):161–177, 2007.
- [9] Ernst Rudolf Georg Eckert and Robert M Drake Jr. Analysis of heat and mass transfer. 1987.
- [10] T. Ferreira. *Influence of the gas-to-wall temperature ratio on bypass transition.* von Karman Institute fo fluid dynamics, Rhode Saint Genese, Belgium, 2016.
- [11] F. Fontaneto. *Aero-thermal performance of a film-cooled high pressure turbine blade / vane: a test case for numerical code validation.* von Karman Institute for Fluid Dynamics, Rhode-St-Genese, Belgium, 2014.

- [12] S. B. Harrison, D. J. Mee, and T. V. Jones. Experiment on the influence of heating on boundary layer transition in favourable pressure gradients. In *Proceedings Eurotherm Seminar*, 1991.
- [13] William Morrow Kays. *Convective heat and mass transfer*. Tata McGraw-Hill Education, 2012.
- [14] R. B. Langtry. *A Correlation-Based Transition Model using Local Variables for Unstructured Parallelized CFD codes*. University of Stuggart, Stuggart, Germany, 2006.
- [15] R. B. Langtry and F. R. Menter. Correlation-based transition modeling for unstructured parallelized computational fluid dynamics codes. *AIAA journal*, 47(12):2894–2906, 2009.
- [16] R. Maffulli and L. He. Impact Of Wall Temperature On Heat Transfer Coefficient And Aerodynamics For 3-D Turbine Blade Passage. *Journal of Thermal Science and Engineering Applications*, 2017.
- [17] M Matsubara and P Henrik Alfredsson. Disturbance growth in boundary layers subjected to free-stream turbulence. *Journal of fluid mechanics*, 430:149–168, 2001.
- [18] F Menter. Zonal two equation kw turbulence models for aerodynamic flows. In *23rd fluid dynamics, plasmadynamics, and lasers conference*, page 2906, 1993.
- [19] F. R. Menter, R. B. Langtry, S. R. Likki, Y. B. Suzen, P. G. Huang, and S. Volker. A correlation-based transition model using local variables Part I: model formulation. *Journal of turbomachinery*, 128(3):413–422, 2006.
- [20] E. Collado Morata, N. Gourdain, F. Duchaine, and L. Y. M. Gicquel. Effects of free-stream turbulence on high pressure turbine blade heat transfer predicted by structured and unstructured LES. *International Journal of Heat and Mass Transfer*, 55(21):5754–5768, 2012.
- [21] S. Ozgen. Effect of heat transfer on stability and transition characteristics of boundary-layers. *International journal of heat and mass transfer*, 47(22):4697–4712, 2004.
- [22] Pierre Ricco. The pre-transitional klebanoff modes and other boundary-layer disturbances induced by small-wavelength free-stream vorticity. *Journal of Fluid Mechanics*, 638:267–303, 2009.
- [23] R.Maffulli. *Conjugate Heat Transfer in High Pressure Turbines*. University of Oxford, Oxford, Uk, 2016.
- [24] P. Schafer, J. Severin, and H. Herwig. The effect of heat transfer on the stability of laminar boundary layers. *International journal of heat and mass transfer*, 38(10):1855–1863, 1995.

- [25] Hermann Schlichting, Klaus Gersten, Egon Krause, Herbert Oertel, and Katherine Mayes. *Boundary-layer theory*, volume 7. Springer, 1960.
- [26] O. Sharma. Momentum and thermal boundary layers on turbine airfoil suction surfaces. In *23rd Joint Propulsion Conference*, page 1918, 1987.
- [27] K. H. Sohn, J. E. OBrien, and E. Reshotko. Some characteristics of bypass transition in a heated boundary layer. In *Turbulent Shear Flows 7*, pages 137–153. Springer, 1991.
- [28] D. Keith Walters and D. Cokljat. A three-equation eddy-viscosity model for Reynolds-averaged Navier Stokes simulations of transitional flow. *Journal of fluids engineering*, 130(12):121401, 2008.
- [29] J. H. Watmuff, D. A. Pook, T. Sayadi, and X. Wu. Fundamental physical processes associated with bypass transition. In *Proceedings of the Summer Program*, page 97, 2010.
- [30] A. PS Wheeler, R. D. Sandberg, N. D. Sandham, R. Pichler, V. Michelassi, and G. Laskowski. Direct numerical simulations of a high-pressure turbine vane. *Journal of Turbomachinery*, 138(7):071003, 2016.